

Regeneration of the entire human epidermis using transgenic stem cells

Tobias Hirsch^{1*}, Tobias Rothoefl^{2*}, Norbert Teig^{2*}, Johann W. Bauer^{3*}, Graziella Pellegrini^{4,5*}, Laura De Rosa^{5*}, Davide Scaglione⁶, Julia Reichelt³, Alfred Klausegger³, Daniela Kneisz³, Oriana Romano⁷, Alessia Secone Seconetti⁵, Roberta Contin⁵, Elena Enzo⁵, Irena Jurman⁸, Sonia Carulli⁹, Frank Jacobsen¹, Thomas Luecke¹⁰, Marcus Lehnhardt¹, Meike Fischer², Maximilian Kueckelhaus¹, Daniela Quaglino⁷, Michele Morgante⁸, Silvio Bicciato⁷, Sergio Bondanza⁹ & Michele De Luca⁵

Junctional epidermolysis bullosa (JEB) is a severe and often lethal genetic disease caused by mutations in genes encoding the basement membrane component laminin-332. Surviving patients with JEB develop chronic wounds to the skin and mucosa, which impair their quality of life and lead to skin cancer. Here we show that autologous transgenic keratinocyte cultures regenerated an entire, fully functional epidermis on a seven-year-old child suffering from a devastating, life-threatening form of JEB. The proviral integration pattern was maintained *in vivo* and epidermal renewal did not cause any clonal selection. Clonal tracing showed that the human epidermis is sustained not by equipotent progenitors, but by a limited number of long-lived stem cells, detected as holoclones, that can extensively self-renew *in vitro* and *in vivo* and produce progenitors that replenish terminally differentiated keratinocytes. This study provides a blueprint that can be applied to other stem cell-mediated combined *ex vivo* cell and gene therapies.

Generalized JEB is a severe and often lethal genetic disease that is characterized by structural and mechanical fragility of the integuments. Blisters and erosions of the skin and mucosa occur within the lamina lucida of the basement membrane in response to minor trauma. Massive chronic skin wounds greatly impair patients' quality of life, lead to recurrent infections and scars, and predispose patients to skin cancer. JEB is caused by mutations in three genes—*LAMA3*, *LAMB3* or *LAMC2*—that jointly encode laminin-332 (a heterotrimeric protein, also known as laminin 5, consisting of $\alpha 3$, $\beta 3$, and $\gamma 2$ chains) and in genes that encode collagen XVII and $\alpha 6\beta 4$ integrins¹. Deleterious mutations that cause an absence of laminin-332 are usually lethal early in life. In nonlethal cases of JEB, laminin-332 is strongly reduced and hemidesmosomes are rudimentary or absent. There is no cure for JEB and more than 40% of patients die before adolescence^{1,2}. The available symptomatic treatments can only relieve the devastating clinical manifestations.

Monthly renewal and timely repair of the human epidermis is sustained by epidermal stem cells, which generate colonies known as holoclones^{3,4}. Holoclones produce meroclone- and paracclone-forming cells, which behave as transient amplifying progenitors^{3,4}. Epithelial cultures harbouring holoclone-forming cells can permanently restore massive skin and ocular defects^{5–9}. A phase I/II clinical trial (one patient) and a single-case study provided compelling evidence that local transplantation of transgenic epidermal cultures can generate a functional epidermis, leading to permanent (the longest follow-up being of 12 years) correction of skin lesions in patients with JEB^{10–12}. However, owing to the paucity of treated areas (a total of around 0.06 m^2), the treatment did not substantially improve the patients' quality of life^{10–12}.

A major criticism of this therapeutic approach has been its supposed unsuitability for the massive skin lesions marking generalized JEB. Here we demonstrate life-saving regeneration of virtually the entire epidermis (approximately 0.85 m^2) of a seven-year-old child suffering from a devastating form of JEB, by means of autologous transgenic keratinocyte cultures. The regenerated epidermis remained robust and resistant to mechanical stress and did not develop blisters or erosions during the 21-month follow-up. This fully functional epidermis is entirely sustained by a limited number of transgenic epidermal stem cells, detected as holoclones, that can extensively self-renew *in vitro* and *in vivo*.

The patient

In June 2015, a seven-year-old child was admitted to the Burn Unit of the Children's Hospital, Ruhr-University, Bochum, Germany. He carried a homozygous acceptor splice site mutation (C1977-1G>A, IVS 14-1G>A) within intron 14 of *LAMB3*. Since birth, the patient had developed blisters all over his body, particularly on his limbs, back and flanks. His condition deteriorated severely six weeks before admission, owing to infection with *Staphylococcus aureus* and *Pseudomonas aeruginosa*. Shortly after admission, he suffered complete epidermal loss on about 60% of his total body surface area (TBSA). During the following weeks, all therapeutic approaches failed and the patient's short-term prognosis was unfavourable (Methods). After the patient's parents had provided informed consent, the regional regulatory authorities and the ethical review board of the Ruhr-University authorized the compassionate use of combined *ex vivo* cell and gene therapy. The parents of the patient also consented

¹Department of Plastic Surgery, Burn Centre, BG University Hospital Bergmannsheil, Ruhr University Bochum, 44789 Bochum, Germany. ²Department of Neonatology and Pediatric Intensive Care, University Children's Hospital, Ruhr University Bochum, 44791 Bochum, Germany. ³EB House Austria and Department of Dermatology, University Hospital of the Paracelsus Medical University, 5020 Salzburg, Austria. ⁴Department of Surgery, Medicine, Dentistry and Morphological Sciences, University of Modena and Reggio Emilia, 41124 Modena, Italy. ⁵Center for Regenerative Medicine "Stefano Ferrari", Department of Life Sciences, University of Modena and Reggio Emilia, 41125 Modena, Italy. ⁶IGA Technology Services s.r.l., 33100 Udine, Italy.

⁷Department of Life Sciences, University of Modena and Reggio Emilia, 41125 Modena, Italy. ⁸Istituto di Genomica Applicata e Dipartimento di Scienze Agroalimentari, Ambientali e Animali, University of Udine, 33100 Udine, Italy. ⁹Holostem Terapie Avanzate s.r.l., 41125 Modena, Italy. ¹⁰Department of Neuropaediatrics, University Children's Hospital, Ruhr University Bochum, 44791 Bochum, Germany.

*These authors contributed equally to this work.



Figure 1 | Regeneration of the transgenic epidermis. **a**, Clinical picture of the patient showing massive epidermal loss. **b**, Schematic representation of the clinical picture. The denuded skin is indicated in red; blistering areas are indicated in green. Flesh-coloured areas indicate currently non-blistering skin. Transgenic grafts were applied on both red and green areas. **c**, Restoration of patient's entire epidermis, with the exception of very few areas on the right thigh, buttocks, upper shoulders/neck and left axilla (white circles, altogether $\leq 2\%$ of TBSA). **d**, Normal skin functionality and elasticity. **e**, Absence of blister formation at sites where post-graft biopsies were taken (arrow).

to the publication of the photographs and medical information included in this paper.

At the time of the first surgery, the patient had complete epidermal loss on approximately 80% TBSA (Fig. 1a, b).

Regeneration of epidermis by transgenic cultures

In September 2015, a 4-cm² biopsy, taken from a currently non-blistering area of the patient's left inguinal region, was used to establish primary keratinocyte cultures, which were then transduced with a retroviral vector expressing the full-length *LAMB3* cDNA under the control of the Moloney leukaemia virus long terminal repeat¹³ (MLV-RV; Methods, Extended Data Fig. 1). Sufficient 0.85-m² transgenic epidermal grafts, enough to cover all of the patient's denuded body surface, were applied sequentially on a properly prepared dermal wound bed (Extended Data Fig. 2a). All limbs, flanks and the entire back were treated with grafts during October and November 2015. Some of the remaining denuded areas received grafts during January 2016.

Previously, transgenic epidermal sheets have been cultivated on plastic, enzymatically detached from the vessel and mounted on a non-adhering gauze^{10–12}. Keratinocyte cultivation on a fibrin substrate—currently used to treat massive skin and ocular burns^{6,8,9}—eliminates cumbersome procedures for graft preparation and transplantation and avoids epidermal shrinkage, allowing the production of larger grafts from the same number of clonogenic cells as are needed to produce plastic-cultured grafts. Because degradation of fibrin after transplantation, which is critical to allow cell engraftment, had never been assessed in a wound bed of a patient with JEB, at the first surgery we compared plastic- and fibrin-cultured grafts (Methods, Extended Data Fig. 1).

The left arm received plastic-cultured grafts (Extended Data Fig. 2b, asterisks). Upon removal of the non-adhering gauze (ten days after grafting, Extended Data Fig. 2c, arrows), epidermal engraftment was evident (asterisks). One month after grafting, epidermal regeneration was stable and complete (Extended Data Fig. 2d). The left leg received both plastic- and fibrin-cultured grafts (Extended Data Fig. 2e, asterisk and arrow, respectively), both of which showed full engraftment after ten days (Extended Data Fig. 2f, asterisk and arrow, respectively) and complete epidermal regeneration after one month (Extended Data Fig. 2f, inset). Similar data were obtained on the other limbs. Thus,

the patient's denuded back (Extended Data Fig. 2g) was treated with only fibrin-cultured grafts (inset). As shown in Extended Data Fig. 2h, virtually complete epidermal regeneration was observed after 1 month, with the exception of some areas (asterisks), some of which contained islands of newly formed epidermis (arrows). Over the following weeks, the regenerated epidermis surrounding the open lesions and the epidermal islands spread and covered most of the denuded areas (Extended Data Fig. 2i). We then transplanted grafts onto the remaining defects on the patient's flanks, thorax, right thigh, right hand and shoulders. Epidermal regeneration was attained in most of those areas.

Thus, approximately 80% of the patient's TBSA was restored by the transgenic epidermis (Fig. 1c). During the 21-month follow-up (more than 20 epidermal renewing cycles), the regenerated epidermis adhered firmly to the underlying dermis, even after induced mechanical stress (Fig. 1d and Supplementary Video), healed normally and did not form blisters, including in areas where follow-up biopsies were taken (Fig. 1e, arrow).

The patient was discharged in February 2016. His epidermis is currently stable and robust, and does not blister, itch, or require ointment or medications.

Ten punch biopsies were taken randomly, 4, 8 and 21 months after grafting. The epidermis had normal morphology and we could not detect blisters, erosions or epidermal detachment from the underlying dermis (Extended Data Fig. 3a). *In situ* hybridization using a vector-specific *t-LAMB3* probe showed that the regenerated epidermis consisted only of transgenic keratinocytes (Fig. 2a). At admission, laminin 332-β3 was barely detectable in the patient's skin (Fig. 2b). By contrast, after grafting, control epidermis (obtained from surgical waste, typically from abdominoplasties or mammoplasty reduction) and transgenic epidermis expressed virtually identical amounts of laminin 332-β3, which was properly located at the epidermis–dermis junction (Fig. 2b). In addition, the basal lamina contained normal amounts of laminin 332-α3 and γ2 chains and α6β4 integrins, all of which had been strongly decreased at admission (Extended Data Fig. 3b). Thus, transduced keratinocytes restored a proper adhesion machinery (Extended Data Fig. 3c). Indeed, the transgenic epidermis showed normal thickness and continuity of the basement membrane (Fig. 2c, arrowheads) and normal morphology of hemidesmosomes (Fig. 2c, arrows). Twenty-one months after surgery, the patient's serum did not contain autoantibodies directed against the basement membrane zone (Extended Data Fig. 3d).

In summary, transgenic epidermal cultures generated an entire functional epidermis in a patient with JEB. This is consistent with the use of keratinocyte cultures for decades to successfully treat victims of life-threatening burns on up to 98% of TBSA^{5,6,9,14}. It can be argued that the patient's clinical picture (massive epidermal loss, critical conditions, poor short-term prognosis) was unusual and our aggressive surgery (mandatory for this patient) unthinkable for the clinical course of most patients with epidermolysis bullosa. However, progressive replacement of diseased epidermis can be attained in multiple, less-invasive surgical interventions on more limited body areas. Epidermolysis bullosa has the advantage of a preserved dermis (not available in deep burns), which allows good functional and cosmetic outcomes. This approach would be optimal for newly diagnosed patients early in their childhood. A bank of transduced epidermal stem cells taken at birth could be used to treat skin lesions while they develop, thus preventing, rather than restoring, the devastating clinical manifestations that arise in these patients through adulthood. Currently, combined *ex vivo* cell and gene therapy cannot be applied to lesions of the internal mucosae; however, such lesions are usually more manageable than those on the skin, perhaps with the exception of oesophageal strictures.

Integration profile of transgenic epidermis

Pre-graft transgenic cultures (PGc) were generated from about 8.7×10^6 primary clonogenic cells and consisted of 2.2×10^8 keratinocytes

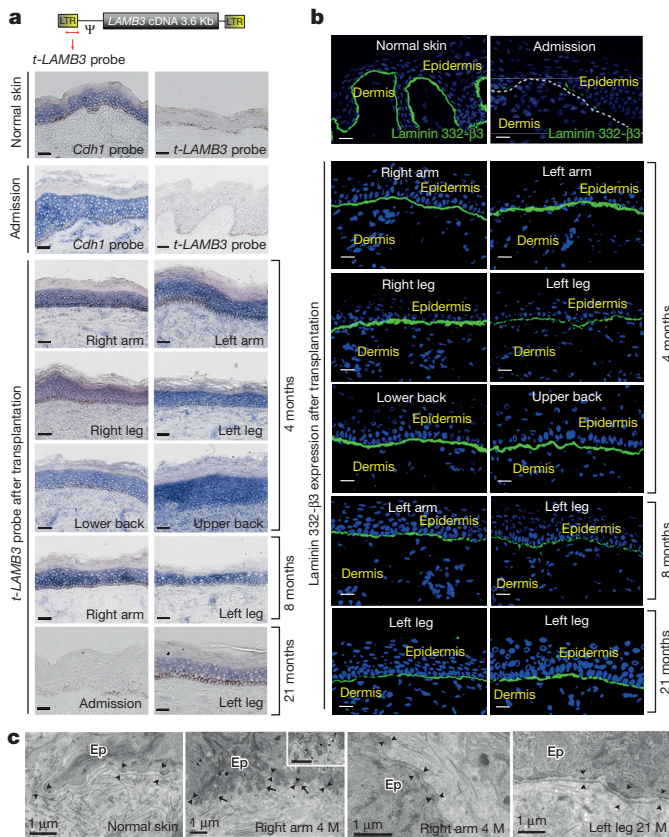


Figure 2 | Restoration of a normal epidermis–dermis junction. Skin sections were prepared from skin from a healthy control subject (surgical waste from abdominoplasties or mammoplasty reduction), the patient's affected skin (admission) and transgenic skin at 4, 8 and 21 months (M) follow-up. **a**, *In situ* hybridization was performed using a transgene-specific probe (*t-LAMB3*) on 10-μm-thick skin sections. An E-cadherin-specific probe (*Cdh1*) was used as a control. Scale bars, 40 μm. **b**, Immunofluorescence for laminin 332-β3 was performed with 6F12 monoclonal antibodies on 7-μm-thick skin sections. DAPI (blue) stains nuclei. Dotted line marks the epidermis–dermis junction. Scale bars, 20 μm. **c**, Electron microscopy was performed on 70-nm-thick skin sections. A regular basement membrane (arrows) and normal hemidesmosomes (arrowheads, higher magnification in the inset) can be seen in sections of the patient's transgenic skin. Scale bars, 1 μm.

(divided into 36 vials), around 45% of which were seeded to prepare 0.85-m² transgenic epidermal grafts (Extended Data Fig. 1).

To investigate the genome-wide integration profile, we sequenced three PGC samples using two independent long terminal repeat (LTR) primers (3pIN and 3pOUT, Supplementary Table 1) for library enrichment ($n=12$; see Methods). High-throughput sequencing recovered a total of 174.9 million read pairs and the libraries obtained using the two LTR primers showed a similar number of reads and comparable insertion counts (Pearson $R>0.92$, $P<0.005$). After merging all integration sites from the two independent priming systems, we identified 27,303 integrations in PGC (Fig. 3a, bars) with an average coverage of 2.5 reads per insertion (Fig. 3a, lines and Supplementary Table 4). The same analysis was performed on primary cultures initiated from three biopsies (approximately 0.5 cm² each) taken four (left leg) and eight (left arm and left leg) months after grafting (4Mc, 8Mc₁, and 8Mc₂, respectively; see Methods).

Notably, we detected only 400, 206, and 413 integrations in 4Mc, 8Mc₁, and 8Mc₂, respectively (Fig. 3a, bars), with average coverage of 27.3, 19.5, and 20.4 reads per insertion (Fig. 3a, lines).

To exclude the possibility that the large difference in the number of integrations between pre- and post-graft samples could be attributable to PCR reactions causing unbalanced representation of event-specific

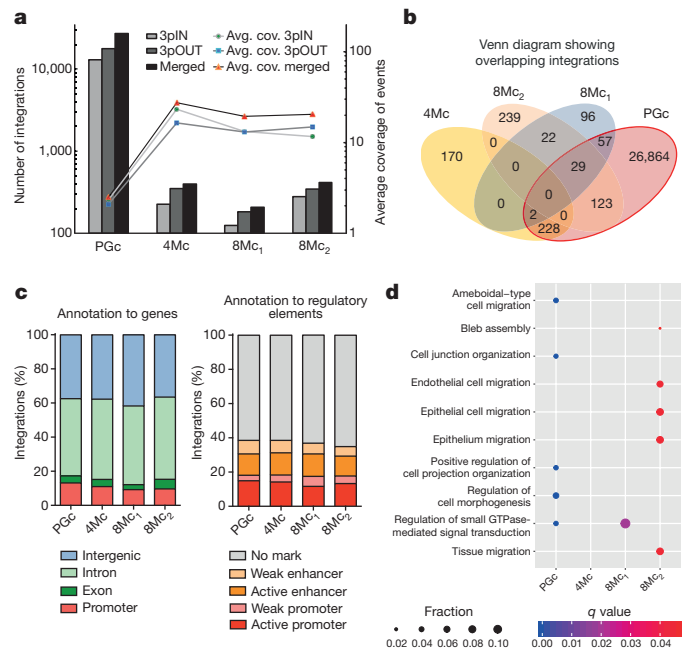


Figure 3 | Integration profile of transgenic epidermis. **a**, Integrations were identified in libraries obtained using two LTR primers (3pIN, light grey bars; 3pOUT, dark grey bars; Supplementary Table 1) and in the merged set (black bars). Lines (right axis) depict the average integration coverage, calculated after removal of PCR duplicates. **b**, Venn diagram of the number of shared integrations across samples. **c**, Percentage of integrations mapped to: promoters, exons, introns, and intergenic regions (left); epigenetically defined active and weak promoters and enhancers, or genomic regions with no histone marks (right). $P>0.05$; Pearson's χ^2 test. **d**, Dot plot of the top five enriched Gene Ontology biological process terms for each sample. Dot colour indicates statistical significance of the enrichment (q value); dot size represents the fraction of genes annotated to each term.

amplicons, or to a spatial effect of punch biopsies, we estimated the expected number of PGC, 4Mc, 8Mc₁, and 8Mc₂ integrations using the Chapman–Wilson capture–recapture model on the data obtained from the independent libraries (Methods)¹⁵. In PGC, the model estimated $65,030 \pm 2,120$ integrations (approximately twice the actual number of detected insertions). The same model estimated 457 ± 31 , 323 ± 50 , and 457 ± 24 independent integrations in 4Mc, 8Mc₁, and 8Mc₂, respectively (confidence level of 99%, $\alpha=0.01$), which is consistent with the number of events detected. Of note, 58%, 43%, and 37% of 4Mc, 8Mc₁, and 8Mc₂ integrations, respectively, were identified in PGC (Fig. 3b), which is consistent with the percentage (approximately 50%) of insertions detected in PGC by next-generation sequencing (NGS) analysis.

Integrations were mapped to promoters (defined as 5-kb regions upstream of the transcription start site of RefSeq genes), exons, introns, and intergenic regions. In all pre- and post-graft samples, about 10% of events were located within promoters. The majority of integrations were either intronic (approximately 47%) or intergenic (approximately 38%) and less than 5% were found in exons (Fig. 3c, left). We also annotated integrations in epigenetically defined transcriptional regulatory elements (Methods). As shown in Fig. 3c (right), about 27% of integrations were associated with active promoters or enhancers and there was no significant difference in the distribution of insertions between pre- and post-graft samples ($P>0.05$; Pearson's χ^2 test). Thus, the integration pattern was maintained *in vivo* and epidermal renewal did not determine any clonal selection.

Genes containing an integration were not functionally enriched in Gene Ontology categories related to cancer-associated biological processes¹⁶, with the exception of cell migration and small GTPase-mediated signal transduction (Fig. 3d and Extended Data Table 1a).

These findings were expected, as our culture conditions were optimized to foster keratinocyte proliferation and migration, to sustain clonogenic cells and to avoid premature clonal conversion and terminal differentiation, all of which are instrumental for the proper clinical performance of cultured epidermal grafts¹⁴. Thus, similar to what has been reported in transgenic haematopoietic stem cells^{17,18}, our high-throughput analyses revealed a cell-specific vector preference that is related to the host cell status in terms of chromatin state and transcriptional activity at the time of transduction¹⁹.

Concerns have been raised about insertional genotoxicity arising from MLV-RV vector use; this has been reported with haematopoietic stem cells in specific disease contexts^{17,20–22}. A γRV vector, similar to ours, obtained marketing authorization for *ex vivo* gene therapy of adenosine deaminase severe combined immunodeficiency and has been approved for phase I/II clinical trials on recessive dystrophic epidermolysis bullosa (RDEB)²³ (<https://clinicaltrials.gov/ct2/show/NCT02984085>).

The patient's integration profile confirmed the absence of clonal selection both *in vitro* and *in vivo*. Likewise, we never observed immortalization events related to specific proviral integrations in many serially cultivated MLV-RV-transduced keratinocytes. Two patients with JEB who received a total of around 1×10^7 clonogenic transgenic keratinocytes at selected body sites (3.5 and 12 years follow-up)^{10–12}, and our patient, who received around 3.9×10^8 transgenic clonogenic cells all over his body (Extended Data Fig. 1), did not manifest tumour development or other related adverse events. Therefore, on the basis of *in vivo* data, the frequency of a detectable transformation event (if any) in MLV-RV-transduced keratinocytes would be less than 1 in 1×10^7 during the first 12 years of follow-up. Although the follow-up of this patient was shorter and does not allow us to draw definitive conclusions, the frequency of detectable insertional mutagenesis events to date is less than 1 in 3.9×10^8 . In evaluating the risk/benefit ratio, it should also be considered that patients with severe JEB are likely to develop aggressive squamous cell carcinoma as a consequence of the progression of the disease.

The transgenic epidermis is sustained by holoclones

The percentage of clonogenic cells, including holoclones, remained relatively constant during the massive cell expansion needed to produce the grafts (Extended Data Fig. 1 and Extended Data Table 2). The patient received approximately 3.9×10^8 clonogenic cells, about 1.6×10^7 of which were holoclone-forming cells, to cover around 0.85 m^2 of his body (Extended Data Figs 1, 4 and Extended Data Table 2). Thus, approximately $4.6 \times 10^4 \text{ cm}^{-2}$ clonogenic cells or approximately $1.8 \times 10^3 \text{ cm}^{-2}$ stem cells were transplanted onto the patient's body surface (Extended Data Fig. 4).

If the originally transduced clonogenic cells were all long-lived equi-potent progenitors, we would have recovered thousands of integrations per cm^2 of regenerated epidermis, and all clonogenic cells contained in 4Mc, 8Mc₁ and 8Mc₂ cultures would have had independent integrations, irrespective of clonal type. Instead, if the transgenic epidermis were sustained by only a restricted number of long-lived stem cells (continuously generating pools of transient amplifying progenitors), we would have recovered, at most, only a few hundred integrations per cm^2 , and meroclones and paraclones contained in 4Mc, 8Mc₁ and 8Mc₂ cultures would have had the same integrations as were found in the corresponding holoclones.

The number of integrations detected in post-graft cultures (Fig. 3a) is consistent with the number of stem cells that have been transplanted (Extended Data Fig. 4), and therefore strongly supports the latter hypothesis, which was verified by proviral analyses at clonal level (Extended Data Fig. 5) on PGc, 4Mc and 8Mc₁. A total of 687 clones (41 holoclones and 646 meroclones or paraclones) were analysed. PGc, 4Mc and 8Mc₁ generated 20, 14 and 7 holoclones and 259, 264 and 123 meroclones or paraclones, respectively. Thus, PGc, 4Mc and 8Mc₁ contained 7.2%, 5.0% and 5.4% holoclone-forming cells, respectively

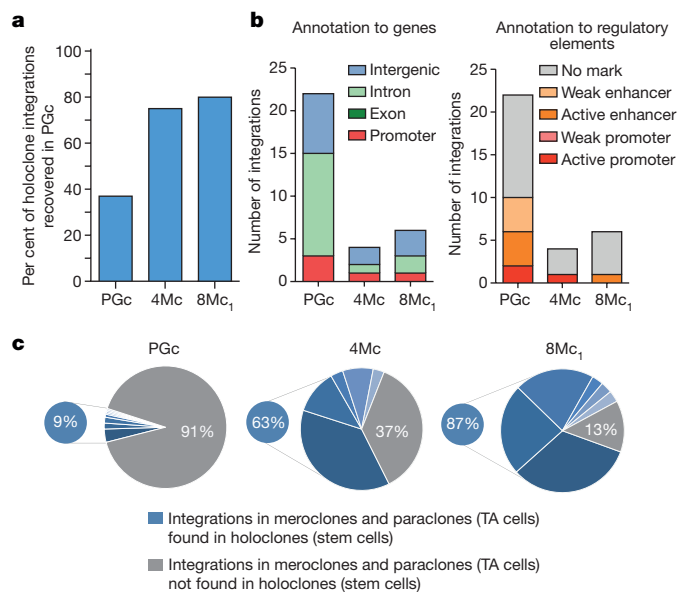


Figure 4 | Integration profile of stem and transient amplifying cells.

a, Percentage of holoclone integrations recovered in the PGc bulk population. b, Holoclone integrations mapped to: promoters, exons, and introns, and intergenic regions (left); epigenetically defined active and weak promoters and enhancers, or genomic regions with no histone marks (right). c, The PGc pie chart shows that 91% of meroclones and paraclones (grey segment) did not contain the same integrations as detected in the corresponding holoclones (each indicated by different blue segments). The 4Mc and 8Mc₁ pie charts show that this percentage decreased to 37% and 13%, respectively. TA, transient amplifying.

(Extended Data Table 2). Each clone was cultivated for further analysis. Libraries of vector–genome junctions, generated by linear-amplification-mediated (LAM) PCR followed by pyrosequencing, retrieved 31 independent integrations unambiguously mapped on the genomes of holoclones (Extended Data Table 1b). One holoclone (4Mc) was untransduced, and 28, 11 and 1 holoclones contained 1, 2 and 3 integrations, respectively. Eleven holoclones in 4Mc shared the same integration pattern. The same happened for two pairs of holoclones in 8Mc₁. The copy numbers of holoclones were confirmed by quantitative PCR with reverse transcription (RT-qPCR) (Extended Data Fig. 6). Notably, 75% and 80% of integrations found in 4Mc and 8Mc₁ holoclones, respectively, were retrieved in PGc (Fig. 4a), supporting the NGS-based survey as well as a representative sampling. The integration pattern observed in holoclones confirms the absence of selection of specific integrations during epidermal renewal *in vivo* (Fig. 4b) and mirrors the pattern found in their parental cultures (Fig. 3c), including the absence of genes associated with cell cycle control, cell death, or oncogenesis (Fig. 3d and Extended Data Table 1a).

We then performed clonal tracing by PCR, using the genomic coordinates of holoclone insertions. As expected, the majority (91%) of PGc meroclones and paraclones did not contain the same integrations as were detected in the corresponding holoclones (Fig. 4c, PGc). This percentage had decreased to 37% by 4 months after grafting (Fig. 4c, 4Mc). Notably, virtually the entire clonogenic population of primary keratinocyte cultures established at 8 months contained the same integrations as were detected in the corresponding holoclones (Fig. 4c, 8Mc₁). Thus, the *in vivo* half-life of transient amplifying progenitors is approximately 3–4 months. These data formally show that the regenerated epidermis is sustained only by long-lived stem cells (holoclones) and underpins the notion that meroclones and paraclones are short-lived progenitors that are continuously generated by the holoclones, both *in vitro* and *in vivo*. The high percentage of holoclone integrations retrieved in PGc, together with the number of shared events across cultures (Fig. 3b), suggests that the average coverage of the NGS analysis in PGc allowed

us to preferentially identify integrations in holoclones and in transient amplifying cells deriving from such holoclones during the cultivation process.

In summary, as depicted in Extended Data Fig. 7, these findings demonstrate that (i) PGc consisted of a mixture of independent transgenic holoclones, meroclones and paraclones; (ii) meroclones and paraclones (which can be isolated directly from a skin biopsy) are transient amplifying progenitors, do not self-renew and are progressively lost during cultivation and *in vivo* epidermal renewal, and therefore do not contribute to the long-term maintenance of the epidermis; (iii) the transgenic epidermis is sustained only by long-lived stem cells detected as holoclones; and (iv) founder stem cells contained in the original primary culture must have undergone extensive self-renewal (*in vitro* and *in vivo*) to ultimately sustain the regenerated epidermis, as confirmed by the number of shared events across samples and across holoclones.

Discussion

The entire epidermis of a patient with JEB can be replaced by autologous transgenic epidermal cultures harbouring an appropriate number of stem cells. Both stem cells and transient amplifying progenitors are instrumental for proper tissue regeneration in mammals²⁴. However, the nature and the properties of mammalian epidermal stem cells and transient amplifying progenitors are a matter of debate^{25,26}. Although epidermal cultures have been used for 30 years in the clinic¹⁴, formal proof of the engraftment of cultured stem cells has been difficult to obtain. Similarly, the identification of holoclones as human epithelial stem cells and of meroclones and paraclones as transient amplifying progenitors, and their role in long-term human epithelial regeneration, have been inferred from compelling but indirect evidence^{6,8,9,27}. Using integrations as clonal genetic marks, we show that the vast majority of transient amplifying progenitors are progressively lost within a few months after grafting and that the regenerated epidermis is sustained only by a limited number of long-lived, self-renewing stem cells. Similar data have been produced with transgenic haematopoietic stem cells²⁸. This notion argues against a model in which a population of equipotent epidermal progenitors directly generate differentiated cells during the lifetime of the animal²⁵, and supports a model in which specific stem cells persist during the lifetime of the human and contribute to both renewal and repair by giving rise to pools of progenitors that persist for various periods of time, replenish differentiated cells and make short-term contributions to wound healing²⁶. Hence, the essential feature of any cultured epithelial graft is the presence (and preservation) of an adequate number of holoclone-forming cells. The notion that the transgenic epidermis is sustained only by engrafted stem cells further decreases the potential risk of insertional oncogenesis.

In conclusion, transgenic epidermal stem cells can regenerate a fully functional epidermis virtually indistinguishable from a normal epidermis, in the absence of related adverse events so far. The different forms of epidermolysis bullosa affect approximately 500,000 people worldwide (<http://www.debra.org>). The successful outcome of this study paves the way for gene therapy to treat other types of epidermolysis bullosa and provides a blueprint that can be applied to other stem cell-mediated combined *ex vivo* cell and gene therapies.

Online Content Methods, along with any additional Extended Data display items and Source Data, are available in the online version of the paper; references unique to these sections appear only in the online paper.

Received 19 June; accepted 10 October 2017.

Published online 8 November 2017.

1. Fine, J. D. et al. Inherited epidermolysis bullosa: updated recommendations on diagnosis and classification. *J. Am. Acad. Dermatol.* **70**, 1103–1126 (2014).
2. Fine, J. D., Johnson, L. B., Weiner, M. & Suchindran, C. Cause-specific risks of childhood death in inherited epidermolysis bullosa. *J. Pediatr.* **152**, 276–280 (2008).

3. Barrandon, Y. & Green, H. Three clonal types of keratinocyte with different capacities for multiplication. *Proc. Natl. Acad. Sci. USA* **84**, 2302–2306 (1987).
4. Pellegrini, G. et al. Location and clonal analysis of stem cells and their differentiated progeny in the human ocular surface. *J. Cell Biol.* **145**, 769–782 (1999).
5. Gallico, G. G. III, O'Connor, N. E., Compton, C. C., Kehinde, O. & Green, H. Permanent coverage of large burn wounds with autologous cultured human epithelium. *N. Engl. J. Med.* **311**, 448–451 (1984).
6. Pellegrini, G. et al. The control of epidermal stem cells (holoclones) in the treatment of massive full-thickness burns with autologous keratinocytes cultured on fibrin. *Transplantation* **68**, 868–879 (1999).
7. Pellegrini, G. et al. Long-term restoration of damaged corneal surfaces with autologous cultivated corneal epithelium. *Lancet* **349**, 990–993 (1997).
8. Rama, P. et al. Limbal stem-cell therapy and long-term corneal regeneration. *N. Engl. J. Med.* **363**, 147–155 (2010).
9. Ronfard, V., Rives, J. M., Neveux, Y., Carsin, H. & Barrandon, Y. Long-term regeneration of human epidermis on third degree burns transplanted with autologous cultured epithelium grown on a fibrin matrix. *Transplantation* **70**, 1588–1598 (2000).
10. Bauer, J. W. et al. Closure of a large chronic wound through transplantation of gene-corrected epidermal stem cells. *J. Invest. Dermatol.* **137**, 778–781 (2017).
11. De Rosa, L. et al. Long-term stability and safety of transgenic cultured epidermal stem cells in gene therapy of junctional epidermolysis bullosa. *Stem Cell Reports* **2**, 1–8 (2013).
12. Mavilio, F. et al. Correction of junctional epidermolysis bullosa by transplantation of genetically modified epidermal stem cells. *Nat. Med.* **12**, 1397–1402 (2006).
13. Markowitz, D., Goff, S. & Bank, A. Construction and use of a safe and efficient amphotropic packaging cell line. *Virology* **167**, 400–406 (1988).
14. De Luca, M., Pellegrini, G. & Green, H. Regeneration of squamous epithelia from stem cells of cultured grafts. *Regen. Med.* **1**, 45–57 (2006).
15. Chapman, D. G. & Robbins, H. Minimum variance estimation without regularity assumptions. *Ann. Math. Stat.* **22**, 581–586 (1951).
16. Hanahan, D. & Weinberg, R. A. Hallmarks of cancer: the next generation. *Cell* **144**, 646–674 (2011).
17. Auti, A. et al. Gene therapy for immunodeficiency due to adenosine deaminase deficiency. *N. Engl. J. Med.* **360**, 447–458 (2009).
18. Biasco, L. et al. Integration profile of retroviral vector in gene therapy treated patients is cell-specific according to gene expression and chromatin conformation of target cell. *EMBO Mol. Med.* **3**, 89–101 (2011).
19. Cavazza, A. et al. Self-inactivating MLV vectors have a reduced genotoxic profile in human epidermal keratinocytes. *Gene Ther.* **20**, 949–957 (2013).
20. Hacein-Bey-Abina, S. et al. Insertional oncogenesis in 4 patients after retrovirus-mediated gene therapy of SCID-X1. *J. Clin. Invest.* **118**, 3132–3142 (2008).
21. Hacein-Bey-Abina, S. et al. A serious adverse event after successful gene therapy for X-linked severe combined immunodeficiency. *N. Engl. J. Med.* **348**, 255–256 (2003).
22. Howe, S. J. et al. Insertional mutagenesis combined with acquired somatic mutations causes leukemogenesis following gene therapy of SCID-X1 patients. *J. Clin. Invest.* **118**, 3143–3150 (2008).
23. Siprashvili, Z. et al. Safety and wound outcomes following genetically corrected autologous epidermal grafts in patients with recessive dystrophic epidermolysis bullosa. *J. Am. Med. Assoc.* **316**, 1808–1817 (2016).
24. Hsu, Y. C., Li, L. & Fuchs, E. Transit-amplifying cells orchestrate stem cell activity and tissue regeneration. *Cell* **157**, 935–949 (2014).
25. Clayton, E. et al. A single type of progenitor cell maintains normal epidermis. *Nature* **446**, 185–189 (2007).
26. Mascré, G. et al. Distinct contribution of stem and progenitor cells to epidermal maintenance. *Nature* **489**, 257–262 (2012).
27. Pellegrini, G. et al. Biological parameters determining the clinical outcome of autologous cultures of limbal stem cells. *Regen. Med.* **8**, 553–567 (2013).
28. Biasco, L. et al. *In vivo* tracking of human hematopoiesis reveals patterns of clonal dynamics during early and steady-state reconstitution phases. *Cell Stem Cell* **19**, 107–119 (2016).

Supplementary Information is available in the online version of the paper.

Acknowledgements Holostem Terapie Avanzate s.r.l. met all costs of GMP production and procedures of transgenic epidermal grafts. This work was partially supported by the Italian Ministry of Education, University and Research (MIUR), no. CTN01_00177_888744; Regione Emilia-Romagna, Asse 1 POR-FESR 2007–13; Fondazione Cassa di Risparmio di Modena; DEBRA Südtirol - Alto Adige; DEBRA Austria; European Research Council (ERC) under the European Union's Horizon 2020 Research and Innovation Program (grant agreement no. 670126-DENOVOSTEM); ERC under the European Union's Seventh Framework Programme (grant agreement no. 294780-NOVABREED); and Epigenetics Flagship project CNR-MIUR grants. We thank H. Green for continuous support; O. Goertz for his contribution to the surgical procedures; the Department of Anaesthesiology, in particular P. Zahn and T. Maecken, and the entire OR staff, in particular S. Taszarski and V. Stroh, for their dedicated perioperative care; the nurses of ward PÄD1 for continuous and devoted assistance; A. Neumayer and J. Frank for technical assistance in defining clone integrations; B. Mussnig for performing indirect immunofluorescence; M. C. Latella for determining

the average number of integrations in pre- and post-graft cultures; M. Forcato for feedback on the bioinformatics analyses; and G. De Santis for control skin specimens.

Author Contributions T.H., T.R., N.T., J.W.B. and G.P. defined strategic procedures and performed transplantation of the transgenic grafts, surgical and medical procedures and clinical follow-up; L.D.R. performed immunofluorescence data and imaging analysis, analysed the data and assembled all input data, prepared the figures and edited the manuscript; D.S., I.J. and M.M. performed integration profiles of transgenic epidermis; R.C., J.R., A.K. and D.K. performed clonal tracing in epidermal cells; O.R. and S.Bi. conducted all bioinformatics analyses; A.S.S. and E.E. performed *in situ* hybridization; S.C. and S.Bo. performed all culture procedures and preparation of genetically modified epidermal graft; F.J., T.L., M.L., M.F. and M.K. carried out the follow-up on the patient; D.Q. performed

electron microscopy analysis; M.D.L. coordinated the study, defined strategic procedures, administered the experiments and wrote the manuscript.

Author Information Reprints and permissions information is available at www.nature.com/reprints. The authors declare competing financial interests: details are available in the online version of the paper. Readers are welcome to comment on the online version of the paper. Publisher's note: Springer Nature remains neutral with regard to jurisdictional claims in published maps and institutional affiliations. Correspondence and requests for materials should be addressed to M.D.L. (michele.deluca@unimore.it).

Reviewer Information *Nature* thanks A. Aiuti, C. Blanpain, D. Streh and the other anonymous reviewer(s) for their contribution to the peer review of this work.

METHODS

Ethics statement. Five weeks after the patient's admission, we considered a palliative treatment, as the clinical situation had deteriorated. The patient's father asked for possible experimental treatments. We informed the parents of the possibility of the transplantation of genetically modified epidermal cultures. With the help of an interpreter, the parents were informed that the aforementioned procedure had been used only on two patients with epidermolysis bullosa and on limited body sites. They were also informed that, given the patient's critical condition, the complexity of the entire surgical procedure needed for the graft application alone could have been lethal. The potential risk of tumour development within the transplant was also discussed. As the parents still expressed their wish to use this experimental procedure, the local research ethics committee of the Medical Faculty of the Ruhr-University Bochum, contacted in July 2015, gave its approval to perform the procedure if the responsible authorities approved the proposed treatment of our patient. We contacted the Paul-Ehrlich-Institut, which referred the request to the District Council of Arnsberg. The District Council of Arnsberg, North Rhine-Westphalia, Germany, which is responsible for the approval of committed treatments with new medical products, authorized the compassionate use of combined *ex vivo* cell and gene therapy in August 2015. The District Council of Duesseldorf, North Rhine-Westphalia, Germany, approved the genetic engineering work according to the Act on Genetic Engineering §9 Abs. 2 GenTG on the basis of the pre-existing approval for the Gene Technology Laboratory Security Level 2, which had been amended to the operating room of the BG University Hospital Bergmannsheil, Ruhr-University Bochum in August 2015.

The entire procedure used to prepare the transgenic epidermis has been previously scientifically reviewed and evaluated by the Italian Ministry of Health and approved by the ethical review board of the University of Modena and Reggio Emilia, both of which approved a phase I/II clinical trial with the same transgenic cultures in June 2015. Similarly, the Austrian regulatory authorities scientifically reviewed and approved two additional clinical trials envisaging the use of very similar transgenic cultures, the only difference being the transgene used in the vector.

All procedures were performed in adherence to the latest available (2008) version of the International Society for Stem Cell Research (ISSCR) Guidelines for the Clinical Translation of Stem Cells. As all legal requirements currently required in Germany to obtain approval for the treatment had been met and the clinical condition of the patient was deteriorating rapidly, we opted to proceed with the life-saving treatment, which was started in September 2015, after obtaining the parents' informed consent. All documents were presented to the parents in German and their native language, translated by an accredited translator. The patient's parents also consented to the publication of the photographs and medical information included in this publication. All photographs were presented to them before they signed the consent forms.

Ethical approval for obtaining normal control skin specimens, patient information sheets, and consent forms were obtained and approved by our institutions (Comitato Etico Provinciale, Prot. N° 2894/C.E.).

Patient, clinical course, surgical, and post-operative procedures. Since birth, the patient had repeatedly developed blisters, upon minor trauma, on his back, limbs and flanks, which occasionally caused chronic wounds persisting for up to one year. Six weeks before the exacerbation, his condition had deteriorated, with the development of massive skin lesions. One day before admission, he developed fever followed by massive epidermal loss. He was admitted to a tertiary care hospital where topical wound care was performed using absorbable foam dressings (Mepilex, Mölnlycke Healthcare). As the patient appeared septic with elevated infection parameters, systemic antibiotic treatment with meropenem and vancomycin was initiated. Severe electrolyte imbalances required parenteral substitution of sodium, potassium, and magnesium. Swabs revealed infection with *S. aureus* and *P. aeruginosa*. Owing to the large wound area and further deterioration of his clinical condition, the patient was transferred to the paediatric burn centre of the Ruhr-University four days later. At admission, he was suffering from complete epidermal loss on approximately 60% of TBSA, affecting all limbs, the back and the flanks. The patient was febrile and cachectic, with a total body weight of 17 kg (below the third percentile) and had signs of poor perfusion, and his C-reactive protein (CRP) level was 150 mg l⁻¹. Antibiotic treatment was continued according to microbiologic assessment with flucloxacilline and ceftazidime. Retrospectively, the diagnosis of staphylococcal scalded skin syndrome was suspected owing to flaky desquamations appearing 10 days after the symptoms began, and *S. aureus* was found on swabs. The iscorEB clinician score²⁹ was 47. We initiated aggressive nutritional therapy by nasogastric tube (1,100–1,300 kcal d⁻¹) and additional parenteral nutrition (700 kcal d⁻¹, glucose 4 g kg⁻¹ d⁻¹, amino acids 3 g kg⁻¹ d⁻¹, fat 1.5 g kg⁻¹ d⁻¹) according to his nutritional demands calculated using the Galveston formula. A necessary intake of about 1,800 kcal d⁻¹ was determined. Vitamins and trace elements were substituted as needed because zinc, selenium,

and other trace elements were below the detection threshold. Beta-adrenergic blockade with propranolol was also started, as with severe burns³⁰. Owing to bleeding during dressing changes and on-going loss of body fluids from the widespread skin erosions, the transfusion of 300 ml packed red blood cells was required every 7–12 days to keep the Hb value above 6–7 g dl⁻¹, and 20 g albumin was given once per week to keep albumin levels above 2.0 g dl⁻¹. Patient care was performed in accordance with the epidermolysis bullosa treatment guidelines³¹. The patient was bathed in povidone-iodine (PVP) solution or rinsed with polyhexanide-biguanide solution (PHMB) under general anaesthesia, first on a daily basis and subsequently every other day. We also used several topical wound dressings and topic antimicrobials, including PHMB gel and PVP ointment, without any substantial effect on wound healing. However, wounds became cleaner and *S. aureus* was no longer detectable for several weeks. The patient had persistent systemic inflammatory response syndrome (SIRS) with spiking fevers, wasting, and high values of acute-phase proteins (CRP, ferritin). He had chronic pain necessitating comprehensive drug management using fentanyl, dronabinol, gabapentin, amitriptyline and NSAIDs. Antibiotic treatment was continued according to swabs taken once weekly; swabs revealed intermittent wound infection with *P. aeruginosa* and, during the course of treatment, *Enterobacter cloacae*, *Enterococcus faecalis* and again *S. aureus*. Treatment was changed biweekly, omitting glycopeptides, carbapenemes and other drugs of last resort, using mainly ceftazidime, cefepime, ampicilline, flucloxacilline, and tobramycin. Owing to the patient's life-threatening condition, we performed an unsuccessful allotransplantation of split-thickness skin grafts taken from his father. Despite initial engraftment, complete graft loss occurred 14 days post-transplantation. Treatment attempts with Suprathel (Polymedics Innovation GmbH), amnion, and glycerol-preserved donor skin (Glyaderm, Euro Tissue Bank) were also unsuccessful. Further treatment attempts were judged to be futile by several experts. After 5 weeks at the intensive care unit, the patient no longer tolerated nutrition via nasogastric or duodenal tube and began to vomit after small amounts of food. Owing to massive hepatosplenomegaly, percutaneous endoscopic gastrostomy or jejunostomy was not feasible. A Broviac catheter was implanted and total parenteral nutrition was begun (1,500 kcal d⁻¹, glucose 14 g kg⁻¹ d⁻¹, amino acids 4 g kg⁻¹ d⁻¹, fat 2 g kg⁻¹ d⁻¹). Following an attempt at increased fat administration via parenteral nutrition, the patient developed pancreatitis, which resolved after fat was omitted from parenteral nutrition for a few days. With this nutritional regimen, the patient's weight remained stable and blood glucose below 150 mg dl⁻¹ was obtained without insulin administration. At this point, palliative care seemed the only remaining option. Because of the very poor short-term prognosis, we decided to start an experimental therapy approach using autologous epidermal stem cell-mediated combined *ex-vivo* cell and gene therapy (see Ethics statement). Transgenic grafts were prepared, free of charge, under Good Manufacturing Practices (GMP) standards by Holostem Terapie Avanzate s.r.l. at the Centre for Regenerative Medicine "Stefano Ferrari", University of Modena and Reggio Emilia, Modena, Italy. In October 2015, we performed the first transplantation of transgenic cultures onto the four limbs and part of the flanks. At that time, the patient was suffering from complete epidermal loss on about 80% of his body and still needed transfusion of 300 ml packed red blood cells every 7–12 days and 20 g albumin once per week to keep the albumin level above 2.0 g dl⁻¹. He continued to suffer from spiking fevers, wasting, and high values of acute-phase proteins (CRP, ferritin). Wounds were colonized with *S. aureus* and *Escherichia coli*. Perioperative antibiotic therapy was performed with flucloxacilline, ceftazidime and ciprofloxacin. Under general anaesthesia, a careful and thorough disinfection with octenidine dihydrochloride (Schuelke & Mayr) and surgical debridement of all limbs and flanks was performed, with both copper sponges and surgical knives. The debrided areas showed good perfusion with intact dermis. After achieving haemostasis using adrenaline-soaked gauze, we washed all debrided areas thoroughly with saline to prevent adrenaline from coming into contact with cultured grafts. Grafts were carefully transplanted onto the denuded, debrided areas and covered with Adaptic, a non-adhering dressing (Systagenix Wound Management) and sterile dressing. Post-operatively, as total immobilization was recommended after the transplantation, the patient was maintained under continuous isoflurane sedation for 12 days using the AnaConDa system (SedanaMedical). A catheter-related bloodstream infection was successfully treated with vancomycin and meropenem. Despite the use of clonidine and propofol, the patient developed a severe delirium after the isoflurane sedation, which was resolved by treatment with levomepromazine. Engraftment was evaluated at 8–14 days. Epidermal regeneration was evaluated at 1 month (see text). Following the first transplantation, regular weekly transfusion of red blood cells and infusion of albumin was no longer necessary. The patient's general condition improved and enteral nutrition became feasible again, with the patient tolerating up to 400 kcal d⁻¹ via nasogastric tube to complement the parenteral nutrition (1,500 kcal d⁻¹, glucose 14 g kg⁻¹ d⁻¹, amino acids 4 g kg⁻¹ d⁻¹, fat 2 g kg⁻¹ d⁻¹)³². In November 2015, a second transplantation was performed on

the dorsum, the buttocks, and small areas on the shoulders and the left hand. These wounds were colonized with *S. epidermidis* and *E. faecium* at the time of transplantation. Antibiotic treatment was done with vancomycin and ceftazidime due to suspected infection of the Broviac catheter. However, owing to the high risk and severe side effects of long-term sedation, the patient was not sedated after the second transplantation. All dressings on the back and the buttocks had to be removed due to infection with *E. faecium* four days after transplantation. Topical antimicrobial therapy using polihexanide was started. On the dorsum, the graft healed in the following four weeks despite the early infection, and a stable skin without blister formation appeared (see text). Four weeks after the second transplantation, the CRP values remained below 100 mg l⁻¹ and the patient was no longer febrile (Extended Data Fig. 8). Complete enteral nutrition became feasible again. The affected body surface area remained below 10% TBSA. In January 2016, we performed a third procedure in a similar fashion to cover the remaining defects on the flanks, thorax, right thigh, right hand, and shoulders. These wounds were colonized with *S. epidermidis*. The transplanted cells engrafted well. The patient was withdrawn from his analgesics. The Broviac catheter was removed and the patient was discharged 7.5 months after admission. At this time, he still had minor defects on the right thigh and the buttocks (Fig. 1 and Extended Data Fig. 2). The iscorEB clinical score was 12. The transplanted skin was clinically stable and not forming blisters. The child returned to regular elementary school in March 2016.

Cell lines. 3T3J2 cell line. Mouse 3T3-J2 cells were a gift from H. Green, Harvard Medical School. A clinical grade 3T3-J2 cell bank was established under GMP standards by a qualified contractor (EUFETS, GmbH), according to ICH guidelines. GMP-certified 3T3-J2 cells have been authorized for clinical use by national and European regulatory authorities and were cultured in Dulbecco's modified Eagle's medium (DMEM) supplemented with 10% irradiated calf serum, glutamine (4 mM) and penicillin–streptomycin (50 IU ml⁻¹).

MFG-LAMB3-packaging cell line. A retroviral vector expressing the full-length 3.6-kb LAMB3 cDNA under the control of the MLV LTR was constructed by cloning 3.6 kb of LAMB3 cDNA (Gene Bank accession Q13751) into an MFG backbone¹³. A 5' fragment of LAMB3 cDNA (563 bp) from the ATG to StuI site was obtained by PCR using as a template the LB3SN plasmid³³. The PCR product was cloned into NcoI and BamHI sites of the MFG vector. The second fragment of LAMB3 cDNA (3,050 bp) was obtained from LB3SN by enzyme digestion from the StuI to XmnI sites and cloned into the MGF at the StuI site. The entire cDNA of LAMB3 was fully sequenced. The Am12-MGF-LAMB3 producer cell lines were generated by transinfection in the amphotropic Gp+envAm12 packaging cell line³⁴. In brief, plasmid DNA was introduced into the GP+E86 ecotropic packaging cell line³⁴ by standard calcium phosphate transfection. Forty-eight hours after transfection, the supernatant was collected and used to infect the amphotropic packaging cell line GP+envAm12 ATCC n° CRL 9641¹³ for 16 h in the presence of 8 µg ml⁻¹ Polybrene. Infected Am12 cells were clonally selected in HXM medium supplemented with 10% FCS, and containing 0.8 mg ml⁻¹ G418 and 0.2 mg ml⁻¹ hygromycin B (Sigma). Single colonies were screened for human LAMB3 production by immunofluorescence using an antibody specific for LAMB3 (6F12 monoclonal antibody from P. Rousselle, CNRS) and for viral titre. The resulting producer cell lines showed a viral titre of 2 × 10⁶ colony-forming units. A master cell bank of a high-titre packaging clone (Am12-LAMB3 2/8) was made under GMP standards by a qualified contractor (Molmed S.p.A) according to ICH guidelines and cultured in DMEM supplemented with 10% irradiated fetal bovine serum, glutamine (2 mM), and penicillin–streptomycin (50 IU ml⁻¹). All certifications, quality tests and safety tests (including detection of viruses and other microorganisms both *in vitro* and *in vivo*) were performed under GMP standards for both cell lines.

Generation of genetically corrected epidermal sheets and graft preparation. Primary cultures were initiated from skin biopsies taken from a non-blistering area of the inguinal region. Transgenic cultured epidermal grafts were prepared under GMP standards by Holostem Terapie Avanzate s.r.l. at the Centre for Regenerative Medicine "Stefano Ferrari", University of Modena and Reggio Emilia. In brief, a 4-cm² skin biopsy was minced and trypsinized (0.05% trypsin and 0.01% EDTA) at 37°C for 3 h. Cells were collected every 30 min, plated (at 2.7 × 10⁴ cells per cm²) on lethally irradiated 3T3-J2 cells (2.66 × 10⁴ cells per cm²) and cultured in 5% CO₂ and humidified atmosphere in keratinocyte growth medium (KGM): DMEM and Ham's F12 medium (2:1 mixture) containing irradiated fetal bovine serum (10%), insulin (5 µg ml⁻¹), adenine (0.18 mM), hydrocortisone (0.4 µg ml⁻¹), cholera toxin (0.1 nM), triiodothyronine (2 nM), glutamine (4 mM), epidermal growth factor (10 ng ml⁻¹), and penicillin–streptomycin (50 IU ml⁻¹). Sub-confluent primary cultures were trypsinized (0.05% trypsin and 0.01% EDTA) at 37°C for 15–20 min and seeded (1.33 × 10⁴ cells per cm²) onto a feeder layer (8 × 10⁴ cells per cm²) composed of lethally irradiated 3T3-J2 cells and producer GP+envAm12-LAMB3 cells¹² (a 1:2 mixture) in KGM. After 3 days of cultivation, cells were collected

and cultured in KGM on a regular 3T3-J2 feeder layer. Sub-confluent transduced cultures were pooled, re-suspended in KGM supplemented with 10% glycerol, aliquoted, and frozen in liquid nitrogen (36 vials, 5 × 10⁶ cells per vial). At each step, efficiency of colony formation by keratinocytes was determined by plating 1,000 cells, fixing colonies with 3.7% formaldehyde 12 days later and staining them with 1% rhodamine B.

For the preparation of plastic-cultured grafts, transduced keratinocytes were thawed and plated (1 × 10⁴ cells per cm²) on 100-mm culture dishes containing lethally irradiated 3T3-J2 cells and grown to confluence in KGM with no penicillin–streptomycin. Grafts were then detached with dispase II, 2.5 mg ml⁻¹ (Roche Diagnostics S.p.A.) and mounted basal side up on sterile non-adhering gauze (Adaptic, Systagenix Wound Management). For fibrin-cultured grafts, fibrin gels were prepared in 144-cm² plates (Greiner) as described^{10,12,35}. Fibrin gels consisted of fibrinogen (23.1 mg ml⁻¹) and thrombin (3.1 IU ml⁻¹) in NaCl (1%), CaCl₂ (1 mM) and aprotinin (1,786 KIU ml⁻¹). Transduced keratinocytes were thawed and plated (1 × 10⁴ cells per cm²) on lethally irradiated 3T3-J2 cells onto the fibrin gels and grown as above. Grafts were washed twice in DMEM containing 4 mM glutamine, and placed in sterile, biocompatible, non-gas-permeable polyethylene boxes containing DMEM and 4 mM glutamine. Boxes were closed, thermo-sealed and packaged into a sealed, sterile transparent plastic bag for transportation to the hospital.

Immunofluorescence, *in situ* hybridization, transmission electron microscopy, haematoxylin and eosin staining and indirect immunofluorescence. The following antibodies were used for immunofluorescence: mouse 6F12 monoclonal antibody to laminin 332-β3, laminin 332-α3 BM165 monoclonal antibody (both from P. Rousselle, CNRS), laminin 332-γ2 D4B5 monoclonal antibody (Chemicon), α6 integrin 450-30A monoclonal antibody and β4 integrin 450-9D monoclonal antibody (Thermo Fisher Scientific).

For immunofluorescence, normal skin biopsies were obtained as anonymized surgical waste, typically from abdominoplasties or mammoplasty reduction, and used as normal control. The patient's skin biopsies were taken randomly, upon agreement with patient information sheets and consent forms, at 4, 8 and 21 months. Skin biopsies were washed in PBS, embedded in Killik-OCT (Bio-Optica) and frozen. Immunofluorescence was performed on 7-µm skin sections (fixed in PFA 3%, permeabilized with PBS/triton 0.2% for 15 min at room temperature and blocked for 1 h at room temperature with BSA 2% in PBS/triton 0.2%) using the previous described antibodies in BSA 2% in PBS/triton 0.2% and added to skin sections for 30 min at 37°C. Sections were washed three times in PBS/triton 0.1% and incubated with Alexa Fluor 488 goat anti-mouse (Life Technologies), diluted 1:2,000 in BSA 2%, PBS/triton 0.2% for 30 min at 37°C. Cell nuclei were stained with DAPI. Glasses were then mounted with Dako Mounting medium and fluorescent signals were monitored under a Zeiss confocal microscope LSM510meta with a Zeiss EC Plan-Neofluar 40×/1.3 oil immersion objective.

To assess the percentage of transduced colonies, 10,000 cells from the sub-confluent transduced PGc pool were plated on a chamber slide and cultivated for 5 days as above. Chamber slides were fixed in methanol 100% for 10 min at -20°C and immunofluorescence analysis was performed as above. Laminin 332-β3 positive colonies were counted under a Zeiss Microscope AXIO ImagerA1 with EC-Plan Neofluar 20×/0.5 objective.

In situ hybridization was performed on 10-µm skin sections. DIG-RNA probe synthesis was performed according to the manufacturer's instructions (Roche, DIG Labelling MIX). Primer pairs with Sp6/T7 promoter sequences (MWG Biotech) were used to obtain DNA templates for *in vitro* transcription. The following vector-specific primers were used: 5'-Sp6-AGTAACGCCATTGGCAAGG-3' (Tm 60°C) and 5'-T7-AACAGAACGGAGCGAAC-3' (Tm 58°C)^{11,12}. OCT sections were fixed in PFA 4% and permeabilized with proteinase K 5 µg ml⁻¹ and post-fixed in PFA 4%. Sections were then incubated in hybridization solution (50% formamide, 4× SSC, yeast RNA 500 µg ml⁻¹, 1× Denhard's solution, 2 mM EDTA, 10% dextran sulfate in DEPC-treated water) at 37°C for 1 h. DIG-probes were diluted in pre-heated hybridization solution at 80°C for 2 min and added to the slice for 20 h at 37°C. Sections were washed, blocked in antibody buffer (1% blocking reagent from Roche in PBS tween 0.1%) containing 10% sheep serum for 1 h at room temperature. Anti-DIG antibody 1:200 was diluted in the same blocking solution and added to the slide for 4 h at room temperature. Signals were developed with BM-Purple solution ON at room temperature until signal reached the desired intensity. Slices were then mounted in 70% glycerol and visualized with Zeiss Cell Observer microscope with EC-Plan Neofluar 20×/0.5 objective.

For transmission electron microscopy, skin biopsies were fixed in 2.5% glutaraldehyde in Tyrode's saline pH 7.2 (24 h at 4°C), post fixed in 1% osmium tetroxide (Electron Microscopy Sciences) for 2 h at room temperature, dehydrated in ethanol and propylene oxide, and embedded in Spurr resin (Polysciences). Ultrathin 70-nm-thick sections were collected on copper grids, stained with uranyl acetate and lead citrate, and observed with a Jeol 1200 EXII (Jeol Ltd) electron microscope.

For haematoxylin and eosin staining, sections ($7\text{ }\mu\text{m}$) were stained with haematoxylin and eosin (Harris haematoxylin for 2 min, running tap water for 1 min, eosin Y for 2 min, 70% ethanol for 1 min, 95% ethanol for 1 min, 100% ethanol for 1 min, two rinses in 100% xylene for 1 min each) and observed with Zeiss Microscope AXIO ImagerA1 with EC-Plan Neofluar $20\times/0.5$ objective.

For indirect immunofluorescence, normal human skin and monkey oesophagus sections (Menarini-Trinity Biotech), were incubated with the patient's plasma (diluted 1:10) or with healthy donor plasma as a negative control. Bound human IgG on monkey oesophagus sections was detected using α -human IgG monkey-adsorbed, FITC-labelled antibody (Inova Diagnostics) and on normal human split-skin sections using α -human IgG, FITC-labelled antibody (Menarini-Trinity Biotech). Positive control sections were stained with a polyclonal rabbit anti-human laminin-332 antibody (Seralab) (1:100), and goat α -mouse IgG FITC (Millipore/Merck) secondary antibody. Mounting medium and fluorescent signals were monitored under an Axio Observer D1 Objektiv LD Plan-NEOFLUAR $20\times/0.4$ Ph2 Korr $\infty/0-1.5$.

Clonal analysis and DNA analysis. Clonal analysis was performed as described³⁴ and shown in Extended Data Fig. 5. Sub-confluent epidermal cultures were trypsinized, serially diluted and plated in 96-well plates (0.5 cells per well). After 7 days of cultivation, single clones were identified under an inverted microscope and trypsinized. One-quarter of the clone was cultured for 12 days onto a 100-mm (indicator) dish, which was then fixed and stained with rhodamine B for the classification of clonal type³. The remaining three-quarters of the clone was cultivated on 24-multiwell plates for genomic DNA extraction and further analysis (Extended Data Fig. 5).

Library preparation and sequencing. Illumina barcoded libraries were obtained from three independent pre-graft cultures (PGc, generated using three vials, each containing $\sim 220,000$ clonogenic keratinocytes) and three post-graft cultures (4Mc, 8Mc₁, and 8Mc₂). For each sample, two tubes with 500 ng genomic DNA were sheared in 100 μl water by applying three sonication cycles of 15 s each in a Bioruptor (Diagenode) to obtain fragments of 300–500 bp. Fragmented DNA was recovered through purification with 0.8 volumes of Agencourt AMPure XP beads, two washing steps with 80% ethanol, and elution in Tris-HCl 10 mM. Repair of DNA ends and A-tailing of blunt ends were both performed using Agilent SureSelect^{XT} reagents (Agilent Technologies), according to the manufacturer's specifications, followed by purification with 1.2 volumes of AMPure XP beads. A custom universal adaptor was generated by annealing Phos-TAGTCCCTTAAGCGGAG-C3 oligo and GTAATACGACTCACTATAGGGCNNNNNCTCGCTTAAGGGACTAT oligo on a thermocycler from 95 °C to 21 °C, with a decrease of 1 °C per min in a 10 mM Tris-HCl, 50 mM NaCl buffer. Ligation of universal adaptor to A-tailed DNA was carried out in a reaction volume of 30 μl with 400 U T4 DNA ligase (New England Biolabs) with the respective T4 DNA ligase buffer 1 \times and 35 pmol dsDNA universal adaptor, incubated at 23 °C for 1 h and at 20 °C for 1 h, and finally heat-inactivated at 65 °C for 20 min. Each ligation product was purified with 1.2 volumes of AMPure XP beads as described above. The eluate of each reaction was split into three tubes to perform independent PCR reactions in order to mitigate reaction-specific complexity reduction. Each tube was amplified by PCR with a combination of I7-index primers (701/702/703), to multiplex samples on the same Illumina sequencing lane, and of two I5 LTR-primer (501/502) to barcode specific enrichments of MLV-LTR sequences (Supplementary Table 1). PCR reactions were carried out in a final volume of 25 μl , with 20 pmoles of each primer and Phusion High-Fidelity master mix 1 \times (New England Biolabs). PCR products were purified with 0.8 volume AMPure XP beads and all amplification products from the same sample (two fragmentations, three PCR reactions) were pooled and quantified on a Bioanalyzer 2100 high sensitivity chip. Paired-end 125-bp sequencing was performed on an Illumina HiSeq2500 (V4 chemistry). Illumina barcodes on the whole Illumina lanes were combined to maintain a minimum Hamming distance of at least three nucleotides. Extraction and de-multiplexing of reads was obtained using CASAVA software (v. 1.8.2) applying a maximum barcode mismatch of one nucleotide and considering the dual indexing of I7-I5 sequences. Reads were processed using the bioinformatics pipeline described in detail below. In brief, reads were first inspected with cutadapt³⁶ to verify specific enrichments, then trimmed using FASTX-Toolkit (http://hannonlab.cshl.edu/fastx_toolkit/) and bbduk2 (<http://jgi.doe.gov/data-and-tools/bbtools/>) to remove adaptors and primers, and mapped to the human genome reference sequence GRCh37/hg19 using BWA MEM³⁷ with default parameters and the -M flag. Finally, the start coordinate of the alignment was used as the putative integration site.

Genomic and functional annotation of integration events. Annotation of integration sites to gene features was performed using the ChIPseeker R package³⁶. Insertion sites were mapped to promoters (defined as 5-kb regions upstream of the transcription start site), exons, and introns of RefSeq genes, and intergenic regions. Functional enrichment in GO biological processes of genes harbouring an integration site was performed using the clusterProfiler R package³⁶, setting a

q value threshold of 0.05 for statistical significance. Annotation of integration sites to epigenetically defined transcriptional regulatory elements was performed with the BEDTools suite³⁸ using publicly available chromatin immunoprecipitation and sequencing (ChIP-seq) data on histone modifications (H3K4me3, H3K4me1, and H3K27ac) in human keratinocyte progenitors (GSE64328)³⁶.

LAM PCR, NGS on holoclones, PCR on mero/paraclonies and integration site analysis. One hundred nanograms of DNA from transduced keratinocytes was used as template for LAM-PCR. The LAM-PCR product was initiated with a 50-cycle linear PCR and digested with two enzymes simultaneously without splitting the DNA amount using 1 μl MseI (5 U μl^{-1}) and 1 μl PstI (5 U μl^{-1}) (Thermo Fisher) and ligation of an MseI restriction site-complementary linker cassette. LAM-PCR was digested with two enzymes simultaneously without splitting the DNA amount. The second enzyme, PstI, was introduced to eliminate the undesired 5'LTR-LAMB3 sequences. The first exponential biotinylated PCR product was captured using magnetic beads and reamplified by a nested second PCR. LAM-PCR primers used for the MLV-LAMB3 vector are in Supplementary Table 2. For the initial LAM-PCR, the 5'-biotinylated oligonucleotide complementary to the 3'-LTR sequence (5'-GGTACCCGTGTATCCAATAA-3') was used for the linear amplification step. The two sequential exponential amplification steps were performed with nested oligonucleotides complementary to the 3'-LTR sequence (5'-GACTTGTGGTCTCGCTGTTCTTGG-3' and 5'-GGTCTCCTCTGAGTGATTGACTACC-3'), each coupled with the oligonucleotides complementary to the linker cassette (Supplementary Table 2). LAM-PCR amplicons were separated on 2% standard agarose gels (Biozym) and the excised bands cloned into the StrataClone PCR Cloning Kit (Agilent Technologies), PCR-purified using High Pure PCR Product Purification Kit (Roche), shotgun cloned, and sequenced by Sanger, or used as unpurified PCR product as template for NGS library preparation. The fragments were end-repaired, adaptor-ligated, nick-repaired and purified using the Ion Plus Fragment Library Kit (Life Technologies). The template preparation and the sequencing run on the machine were also performed according to the protocols of Life Technologies. A mean vertical coverage was planned to reach at least 2,000 reads.

Screening of the integration sites of the meroclones and paraclonies was done by PCR using a combination of the forward primer MLV 3'LTR control F (5'-GGACCTGAAATGACCCTGTG-3') of the LTR and a specific reverse primer (Supplementary Table 3) in the proximity of the integration site. Genomic DNA from the holoclones was used as positive controls.

Provirus copy number. TaqMan PCR analysis was performed with TaqMan Universal PCR Master Mix and vector-specific *LAMB3* and *GAPDH* probes (*LAMB3*: Hs00165078_m1; *GAPDH*: Hs03929097_g1, Applied Biosystems). The amplicon for *LAMB3* was located between adjacent exons to recognize only provirus *LAMB3*. Reactions were performed with ABI Prism 7900 Sequence Detection System (Applied Biosystems), using 10 ng genomic DNA. The relative quantity that relates to the PCR signal of the target provirus was normalized to the level of *GAPDH* (internal control gene) in the same genomic DNA by using the $2^{-\Delta\Delta C_t}$ quantification.

Bioinformatics analysis of sequencing data. To process the sequencing reads we assembled a custom bioinformatics pipeline composed of standard tools for NGS data analysis. In particular, we first used cutadapt (v.1.14; <https://cutadapt.readthedocs.io/en/stable/>)³⁶ to verify the presence, in read pairs, of specific sequences indicative of a successful enrichment. Specifically, in the read harbouring the I5 LTR-primer sequence (read 1), we searched for the primer sequence and, at its 3'-end, for the remainder LTR sequence. In the read harbouring the I7 indexing primer (read 2), we searched for the presence of the common adaptor sequence preceding the six indexing bases. Pairs containing both sequences were retained for analysis after trimming the I5 primer and the remainder LTR sequence in read 1 and the common adaptor sequence in read 2. Then, we used FASTX-Toolkit (http://hannonlab.cshl.edu/fastx_toolkit/) to remove from read 2 the first six indexing bases, used as a de-duplicator component during de-multiplexing. As half of the amplification products are expected to be non-informative in the detection of the insertion site, given the identity of the two LTRs of the MLV genome, we applied bbduk2 (<http://jgi.doe.gov/data-and-tools/bbtools/>) to identify and remove read pairs representing inward-facing LTR primer enrichment events. In bbduk2 we set the kmer length to 27 ($k=27$) and the edit distance and the maxbadkmers parameter both to 1. Reads were aligned on the human genome reference sequence GRCh37/hg19 using BWA MEM³⁷ with default parameters and the -M flag (to include the multiple-mapping signature in the BAM file). Read pairs sharing the same mapping coordinates and the same de-duplicator component were labelled as PCR duplicates and removed. Aligned read pairs were further filtered to retain only those mapping at a distance between 150 and 600 bp (corresponding to the expected library insert size), allowing a maximum of 1 bp soft-clip (unaligned) on all ends, with the exception of the 5' end of read 2 where we allowed 20 bp soft clip because it contains the 18-bp untrimmed common adaptor

sequence. Finally, we retained read 1 sequences with a minimum mapping quality of 40 and extracted and counted the alignment coordinates of their first base, representing the putative insertion site. Insertion sites within 10 bp of one another were treated as a single insertion, their counts summed using BEDTools (v2.15; <http://bedtools.readthedocs.io/en/latest/content/bedtools-suite.html>)³⁸, and the summed count assigned to the left coordinate. When intersecting insertion sites across samples, we considered overlapping those insertion events closer than 30 bp. **Calculation of the expected number of integrations.** The expected number of integrations (that is, the expected population size) in PGc, 4Mc, 8Mc₁, and 8Mc₂ samples was calculated in R by applying a capture–recapture model based on Chapman's estimate and its confidence intervals^{15,39}:

$$\hat{N} = \frac{(n_1 + 1)(n_2 + 1)}{n_{11} + 1} - 1$$

$$\hat{N} \pm Z_{1-\alpha/2} \sqrt{\frac{(n_1 + 1)(n_2 + 1)n_{21}n_{12}}{(n_{11} + 1)^2(n_{11} + 2)}}$$

where \hat{N} is the estimated number of integrations, n_1 is the number of integrations found in the 3pIN library, n_2 those found in the 3pOUT library, n_{11} the number of overlapping integrations, n_{12} and n_{21} the insertion exclusive of 3pIN and 3pOUT, respectively, and $Z_{1-\alpha/2} = 2.56$ for $\alpha = 0.01$.

Genomic and functional annotation of insertion events. To annotate the integration sites to gene features, we used the ChIPseeker R package (v.1.10.3, <https://bioconductor.org/packages/release/bioc/html/ChIPseeker.html>)⁴⁰. The integration sites were mapped to promoters, defined as 5-kb regions upstream of transcription start sites (TSS), exons, and introns of RefSeq genes, and to intergenic regions.

We performed functional annotation of genes harbouring an integration sites using the clusterProfiler R package (v3.2.14; <https://bioconductor.org/packages/release/bioc/html/clusterProfiler.html>)⁴¹, setting a q value threshold of 0.05 to define enriched GO biological processes.

To annotate the integration sites to epigenetically defined transcriptional regulatory elements (promoters and enhancers), we used the BEDTools suite (v.2.15; <http://bedtools.readthedocs.io/en/latest/content/bedtools-suite.html>)³⁸. We defined promoters and enhancers using publicly available ChIP-seq data on histone modifications (H3K4me3, H3K4me1 and H3K27ac) produced in human keratinocyte progenitors⁴². In brief, BED files containing the coordinates of genomic regions enriched for each histone modification (peaks) were downloaded from the Gene Expression Omnibus database (GSM1568245 for H3K4me3, GSM1568244 for H3K4me1 and GSM1568247 for H3K27ac). H3K4me3 peaks close to the TSS (<5 kb) of RefSeq genes were defined as promoters, whereas H3K4me1 peaks far from the TSS (>5 kb) were defined as enhancers. Promoters and enhancers were classified as 'active' if they overlap with H3K27ac peaks and otherwise as 'weak'. Finally, integration sites were mapped to active and weak promoters and enhancers.

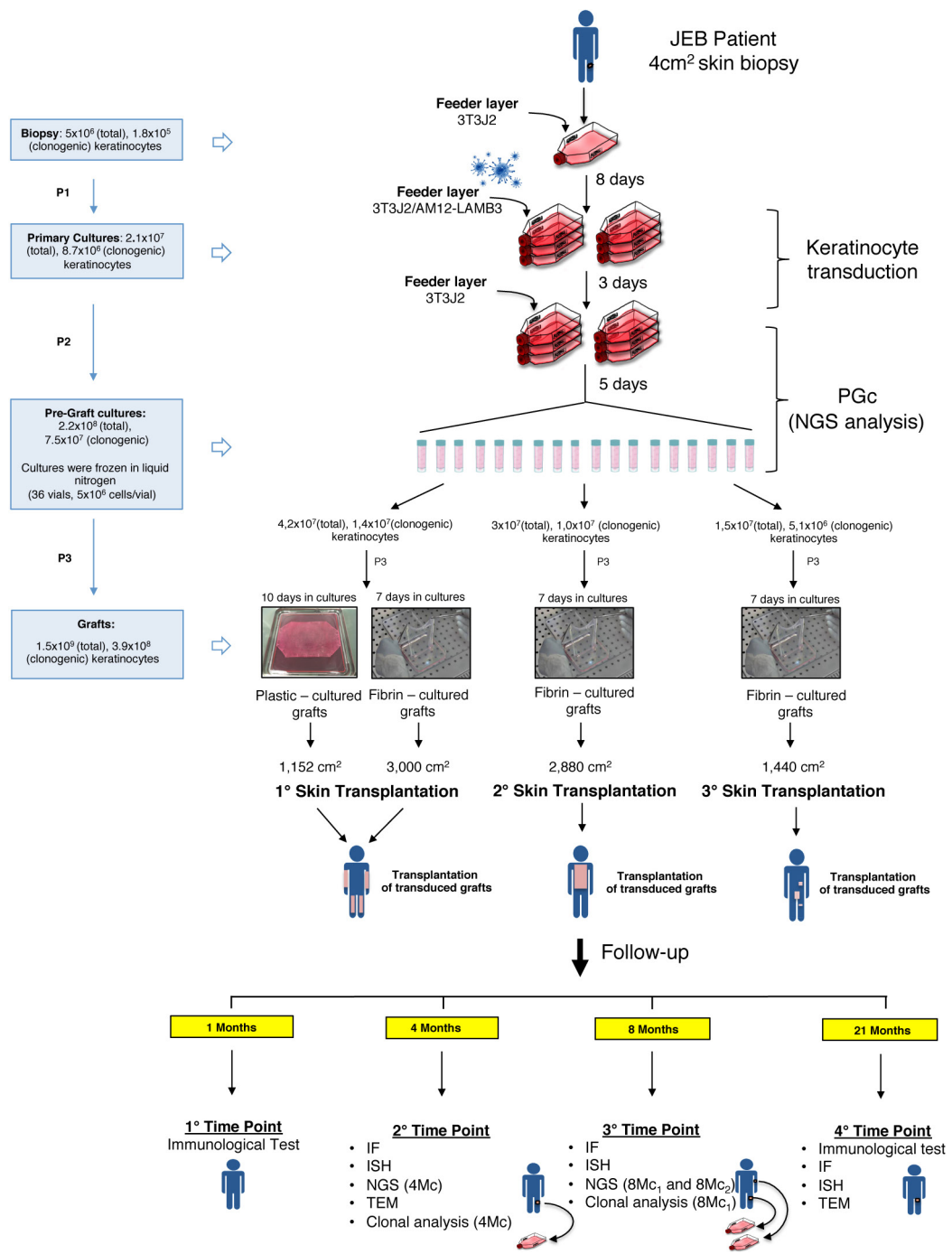
Differences in the annotation of integration sites to gene features and regulatory elements were tested using the chisq.test function (Pearson's χ^2 test) of the stat R package.

Bioinformatics analysis of NGS data from holoclones. Analysis of the data was implemented with single read sequences of the BAM file. Output results with $\geq 5\%$

of query cover, $\geq 95\%$ identity, and a size of ≥ 48 bp were taken into account for confirmation as integration sites with control PCR. Sequences were aligned to the human genome (Genome Reference Consortium GRCh37) using NCBI BLAST (<https://blast.ncbi.nlm.nih.gov/Blast.cgi>). Identification of the nearest gene was performed with dedicated PERL scripts. Visualization of the Retroviral Tagged Cancer Gene Database (RTCGD) CIS integrations as a feature on the UCSC BLAT output was achieved by connecting to UCSC through the RTCGD web interface⁴³ (<http://rtcgd.abcc.ncifcrf.gov>); the map position of each of the retroviral integrations was automatically loaded as custom tracks on the UCSC BLAT search engine. **Statistical analyses and data visualization.** Statistical analyses were implemented in R (v.3.3.1, <http://www.r-project.org/>). Fig. 3d was generated using the ggplot2 R package (v2.2.1, <https://cran.r-project.org/web/packages/ggplot2/index.html>). No statistical methods were used to predetermine sample size. The experiments were not randomized and the investigators were not blinded to allocation during experiments and outcome assessment.

Data availability. All high-throughput sequencing data for the integration profiles have been deposited in the Sequence Read Archive (SRA) under accession number SRR110373. All data used to generate Figs 3, 4 and Extended Data Figs 6, 8 are provided as Source Data.

29. Schwieger-Briel, A. et al. Instrument for scoring clinical outcome of research for epidermolysis bullosa: a consensus-generated clinical research tool. *Pediatr. Dermatol.* **32**, 41–52 (2015).
30. Herndon, D. N. et al. Long-term propranolol use in severely burned pediatric patients: a randomized controlled study. *Ann. Surg.* **256**, 402–411 (2012).
31. Goldschneider, K. R. et al. Pain care for patients with epidermolysis bullosa: best care practice guidelines. *BMC Med.* **12**, 178 (2014).
32. Rodriguez, N. A., Jeschke, M. G., Williams, F. N., Kamolz, L. P. & Herndon, D. N. Nutrition in burns: Galveston contributions. *JPN J. Parenter. Enteral Nutr.* **35**, 704–714 (2011).
33. Dellambra, E. et al. Corrective transduction of human epidermal stem cells in laminin-5-dependent junctional epidermolysis bullosa. *Hum. Gene Ther.* **9**, 1359–1370 (1998).
34. Mathor, M. B. et al. Clonal analysis of stably transduced human epidermal stem cells in culture. *Proc. Natl. Acad. Sci. USA* **93**, 10371–10376 (1996).
35. Guerra, L. et al. Treatment of "stable" vitiligo by timed surgery and transplantation of cultured epidermal autografts. *Arch. Dermatol.* **136**, 1380–1389 (2000).
36. Martin, M. Cutadapt removes adapter sequences from high-throughput sequencing reads. *EMBnet.journal* **17**, 10–12 (2011).
37. Li, H. Aligning sequence reads, clone sequences and assembly contigs with BWA-MEM. Preprint at <https://arxiv.org/abs/1303.3997> (2013).
38. Quinlan, A. R. BEDTools: the Swiss-army tool for genome feature analysis. *Curr. Protoc. Bioinformatics* **47**, 11–34 (2014).
39. Chapman, D. G. *Some Properties of the Hypergeometric Distribution with Applications to Zoological Sample Censuses* (Univ. California Press, 1951).
40. Yu, G., Wang, L. G. & He, Q. Y. ChIPseeker: an R/Bioconductor package for ChIP peak annotation, comparison and visualization. *Bioinformatics* **31**, 2382–2383 (2015).
41. Yu, G., Wang, L. G., Han, Y. & He, Q. Y. clusterProfiler: an R package for comparing biological themes among gene clusters. *OMICS* **16**, 284–287 (2012).
42. Cavazza, A. et al. Dynamic transcriptional and epigenetic regulation of human epidermal keratinocyte differentiation. *Stem Cell Reports* **6**, 618–632 (2016).
43. Akagi, K., et al. RTCGD: retroviral tagged cancer gene database. *Nucleic Acids Res.* **32**, 523–527 (2004).



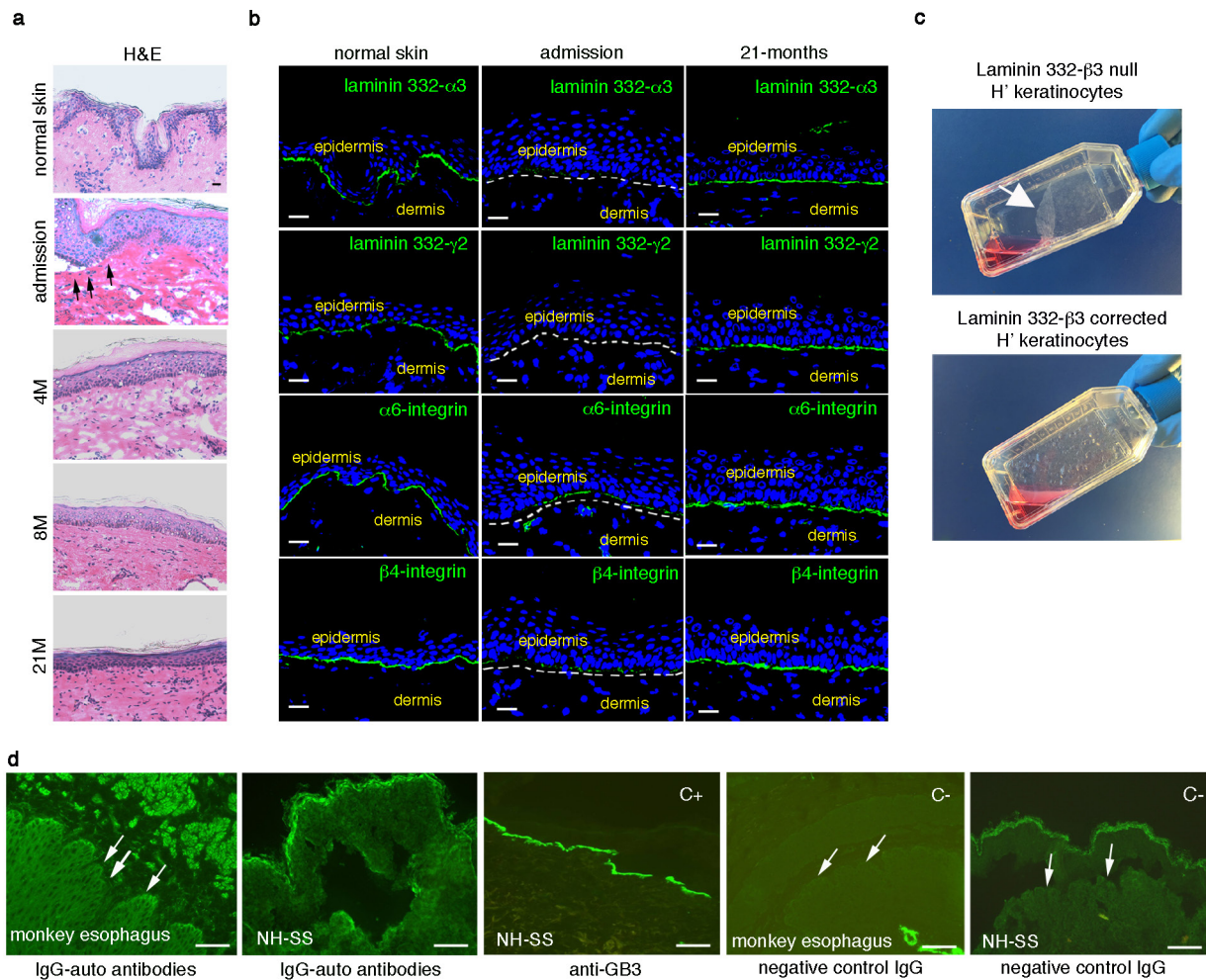
Extended Data Figure 1 | Schematic representation of combined *ex vivo* cell and gene therapy. The scheme shows the entire procedure, from skin biopsy to transplantation and follow-up. The total number of keratinocytes, corresponding clonogenic fraction and days of cultivation are shown for each passage. All analyses performed at each follow-up are indicated. Immunofluorescence (IF), *in situ* hybridization (ISH) and

transmission electron microscopy (TEM) were performed on randomly taken 0.2–0.4-mm² punch biopsies. Genome-wide analysis (NGS) was performed on pre-graft cultures (PGc) and on primary cultures initiated from approximately 0.5-cm² biopsies taken from the left leg (4Mc and 8Mc₂) and the left arm (8Mc₁). Clonal analysis and tracing were performed on PGc, 4Mc and 8Mc₁.



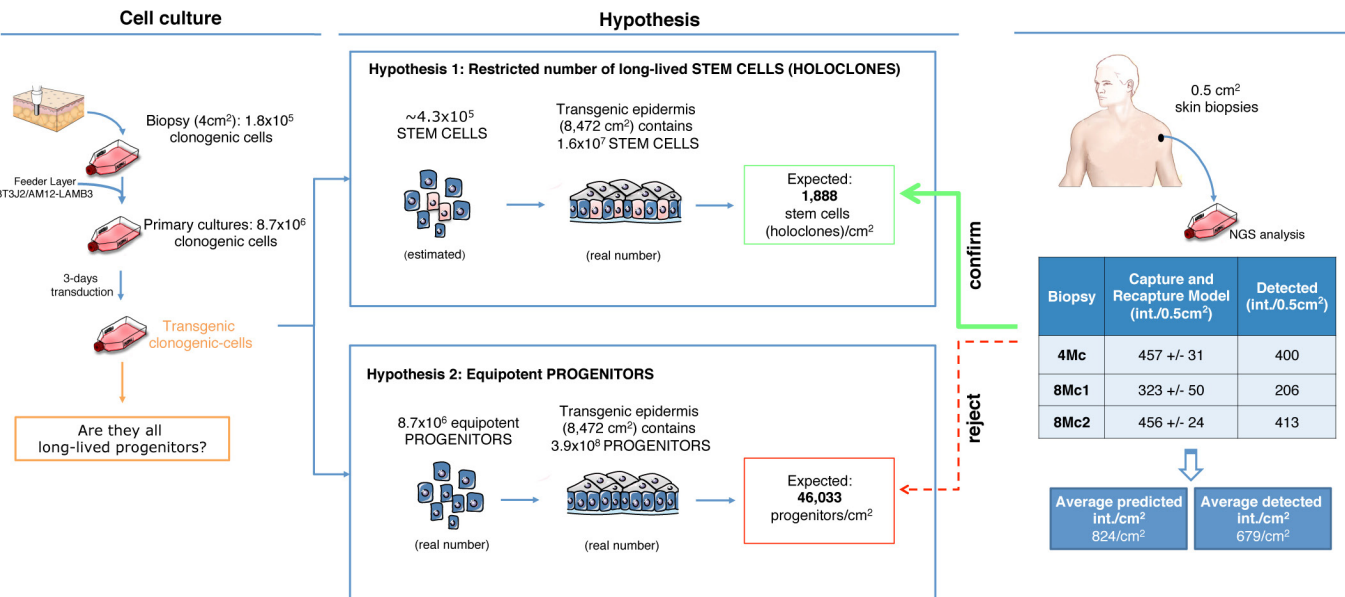
Extended Data Figure 2 | Regeneration of the epidermis by transduced keratinocyte cultures. **a**, Preparation of a dermal wound bed at the time of transplantation. **b**, Transplantation onto the left arm of plastic-cultured epidermal grafts, mounted on a non-adhering gauze (asterisks). **c**, The engrafted epidermis (asterisks) is evident upon removal of the gauze (arrows) ten days after grafting. **d**, Regenerated epidermis on the left arm after 1 month. **e**, **f**, Transplantation (**e**) and engraftment (**f**) of both plastic-cultured (asterisk) and fibrin-cultured (arrow and inset in **e**) grafts on the

left leg. **f**, Inset, complete epidermal regeneration is evident after 1 month. **g**, The back of the patient was covered with fibrin-cultured grafts (inset). **h**, Complete epidermal regeneration was observed after 1 month, with the exception of areas marked with asterisks. Islands of epidermis were observed inside those denuded areas (arrows). **i**, Within 4 months, the regenerated epidermis surrounding the open lesions and the epidermal islands detected within those open lesions had spread and covered the denuded areas.



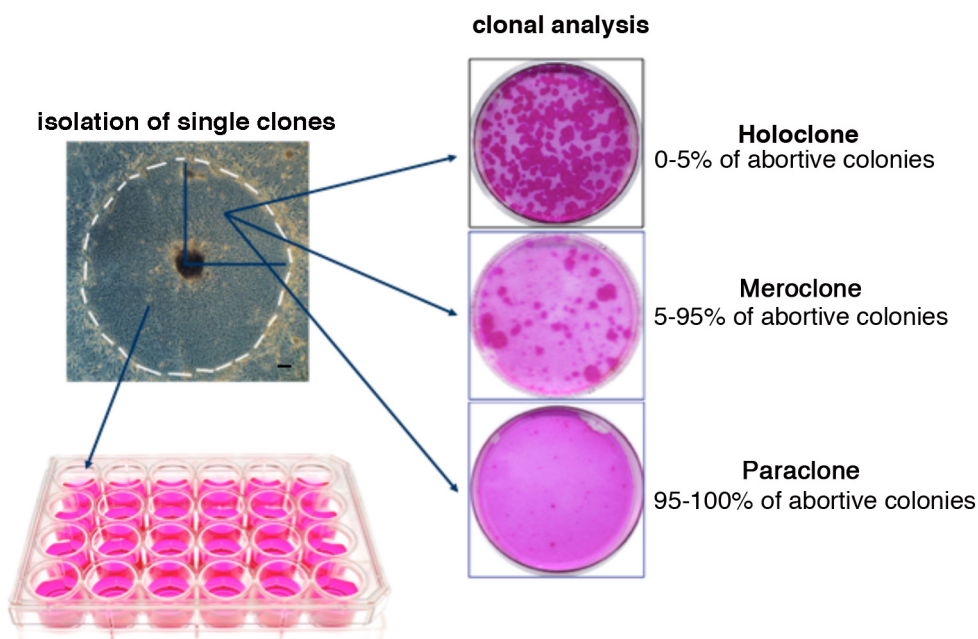
Extended Data Figure 3 | Restoration of a normal dermis–epidermis junction. **a**, Haematoxylin and eosin staining of skin sections (7- μ m thick) prepared from normal skin and from the patient at admission and at 4, 8 and 21 month follow-ups. Black arrows show ruptures at the epidermis–dermis junction. Scale bar, 20 μ m. **b**, Sections (7- μ m thick) from normal skin, the patient's skin at admission and the patient's skin 21 months after transplantation were immunostained using antibodies against laminin 332- α 3, laminin 332- γ 2, α 6 integrin and β 4 integrin. **c**, Adhesion of cohesive cultured epidermal sheets. Top, spontaneous detachment (arrow) of confluent culture of laminin 332- β 3 null keratinocytes from the patient.

Bottom, culture of patient's genetically corrected keratinocytes remained firmly attached to the substrate. As with normal control cells, detachment would have required prolonged enzymatic treatment. **d**, The absence of a humoral immune response to the transgene product was verified by indirect immunofluorescence performed on monkey oesophagus and normal human split skin (NH-SS) sections, using the patient's plasma taken 21 months after transplantation. An anti-human laminin-332 antibody (anti-GB3) was used as a positive control (C+). A healthy donor's plasma was used as negative control (C-). Arrows denote the expected localization of the laminin-332 labelling. Scale bar, 100 μ m.



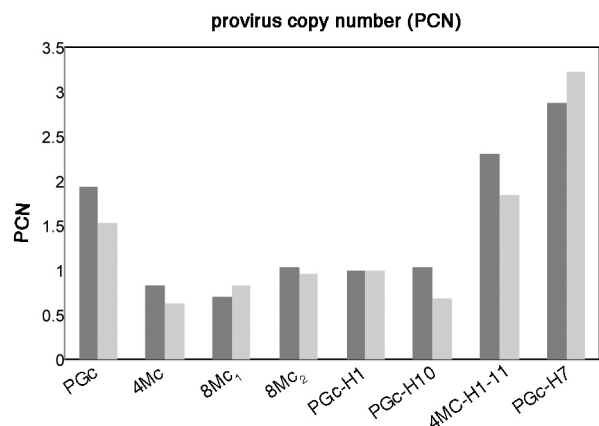
Extended Data Figure 4 | Schematic model of epidermal stem and progenitor cell function. Clonogenic progenitors (blue cells) contained in the original skin biopsy and in $8,472\text{ cm}^2$ of transgenic epidermis are indicated. Stem cells, detected as holoclones (pink cells), were identified by clonal analysis (Methods and Extended Data Fig. 5). The number of holoclones contained in the primary culture has been estimated. The schematic model posits the existence of specific long-lived stem

cells generating pools of short-lived progenitors (Hypothesis 1) or a population of equipotent epidermal progenitors (Hypothesis 2). The number of integrations predicted by the Chapman–Wilson capture–re-capture model and formally detected by NGS analysis in 4Mc, 8Mc₁ and 8Mc₂ (right) is consistent with the number of transplanted holoclones and therefore supports Hypothesis 1.

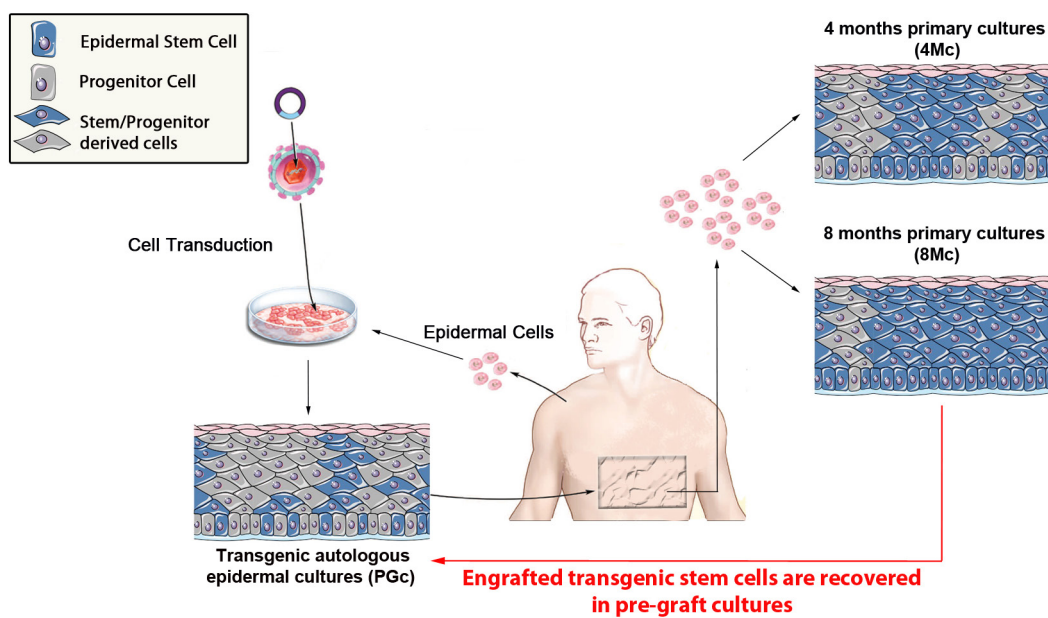


Extended Data Figure 5 | Clonal analysis scheme. Sub-confluent cultures were trypsinized, serially diluted and inoculated (0.5 cells per well) onto 96-multiwell plates containing irradiated 3T3-J2 cells. After 7 days of cultivation, single clones were identified under an inverted microscope (scale bar, 100 μm), trypsinized, transferred to two dishes and cultivated. One dish (one-quarter of the clone) was fixed 12 days later and stained with rhodamine B for the classification of clonal type. The clonal type was

determined by the percentage of aborted colonies formed by the progeny of the founding cell. The clone was scored as a holoclone when 0–5% of colonies were terminal. When 95–100% of colonies were terminal (or when no colonies formed), the clone was classified as a paracclone. When the amount of terminal colonies was between 5% and 95%, the clone was classified as a meroclone. The second dish (three-quarters of the clone) was used for integration analysis after 7 days of cultivation.

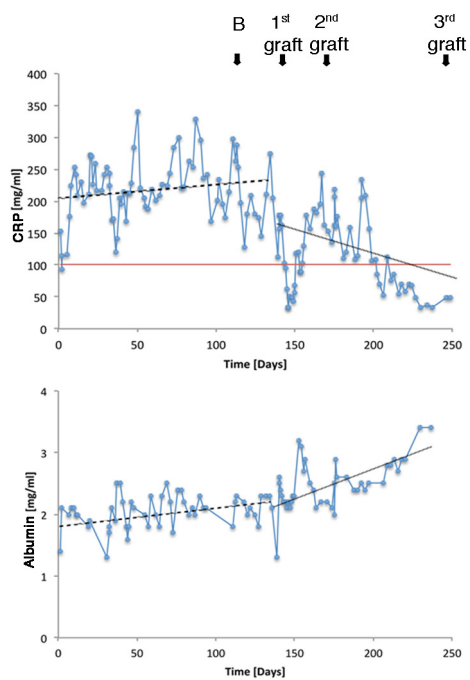
**Extended Data Figure 6 | Determination of provirus copy number.**

Quantitative PCR was performed on genomic DNA from pre-graft cultures (PGC), primary cultures generated at 4 months (4Mc) and 8 months (8Mc₁, 8Mc₂) follow-up and selected holoclones (PRE.G_H1, PRE.G_H10, FU4m_H1-11, PRE.G_H7). The experiment was performed in duplicate and the plot is presented as two individual data points for each sample.



Extended Data Figure 7 | Schematic model of holoclone tracing in the regenerated patient's epidermis. Transgenic epidermal cultures (PGc) contain a mixed population of clonogenic basal stem cells (blue) and transient amplifying progenitors (grey). Upon engraftment and initial epidermal regeneration, both stem and transient amplifying cells can proliferate and eventually generate suprabasal terminally differentiated

cells. Upon epidermal renewal (after 4 and 8 months), the short-lived transient amplifying progenitors (grey) are progressively lost. The long-lived stem cells then generate new pools of transient amplifying progenitors (now blue basal cells), which will produce terminally differentiated cells (suprabasal blue cells).



Extended Data Figure 8 | Clinical data. During his time in hospital, the patient's inflammatory and nutritional status was documented by blood concentration of C-reactive protein (CRP; upper panel) and albumin (lower panel). The times of biopsy sampling (B) and epidermal culture transplantation are shown with arrows. The linear regressions visualize the trend of pre-graft (dotted) and post-graft (black line) progressions. The red line within the CRP time course demonstrates the CRP limit, which is considered a criterion for severe inflammation. These data demonstrate the critical situation of the patient at admission and before transplantation and the improvement of his general status upon epidermal regeneration.

Extended Data Table 1 | Gene Ontology (GO) analysis and genomic and functional annotation of holoclones' integrations

a

Cancer-related biological process	GO ID	Description	q-value (FDR)			
			PGc	4Mc	8Mc ₁	8Mc ₂
Cell death and apoptosis	GO:0070265	necrotic cell death	0.28	0.58	0.56	0.65
	GO:0010939	regulation of necrotic cell death	0.31	0.53	0.53	0.64
	GO:0097300	programmed necrotic cell death	0.25	0.54	0.53	0.66
	GO:2001233	regulation of apoptotic signaling pathway	---	0.52	0.67	0.72
	GO:0006282	regulation of DNA repair	0.06	0.67	---	---
DNA repair	GO:0006298	mismatch repair	0.53	0.54	---	0.66
	GO:0006302	double-strand break repair	0.64	0.57	0.72	0.91
	GO:0006289	nucleotide-excision repair	0.82	0.75	---	0.83
	GO:0036297	interstrand cross-link repair	0.84	0.58	---	0.72
Angiogenesis	GO:0001525	angiogenesis	9.54E-05	0.52	0.59	0.74
	GO:0045765	regulation of angiogenesis	0.53	0.73	0.73	0.72
	GO:0090130	tissue migration	7.82E-06	0.50	0.53	0.04
Migration	GO:0090132	epithelium migration	3.64E-06	0.50	0.53	0.04
	GO:0010631	epithelial cell migration	3.26E-06	0.49	0.53	0.04
	GO:0010632	regulation of epithelial cell migration	2.43E-06	0.44	0.53	0.05
	GO:0051546	keratinocyte migration	0.22	---	0.53	0.65
	GO:0001667	ameboidal-type cell migration	3.19E-08	0.52	0.53	0.06
Inflammation	GO:0002526	acute inflammatory response	0.85	0.58	0.63	---
	GO:0002544	chronic inflammatory response	0.82	0.45	---	---
	GO:0050727	regulation of inflammatory response	0.80	0.69	0.61	0.80
Telomerase activity	GO:0000723	telomere maintenance	0.48	0.77	0.63	0.72
	GO:0007004	telomere maintenance via telomerase	0.38	---	---	0.73
	GO:0032204	regulation of telomere maintenance	0.69	---	---	0.65
Cell cycle	GO:0051972	regulation of telomerase activity	0.66	---	---	---
	GO:0000075	cell cycle checkpoint	0.14	0.60	0.74	---
	GO:1901976	regulation of cell cycle checkpoint	0.18	---	---	---
	GO:1901987	regulation of cell cycle phase transition	0.02	0.48	0.83	---
	GO:0045786	negative regulation of cell cycle	0.01	0.57	0.60	---
Proliferation	GO:0050673	epithelial cell proliferation	4.06E-03	0.52	0.65	0.75
	GO:0050678	regulation of epithelial cell proliferation	0.01	0.52	0.60	0.72
	GO:0043616	keratinocyte proliferation	1.24E-03	0.56	0.55	---
	GO:0010837	regulation of keratinocyte proliferation	0.01	0.54	0.53	---
Glycolysis	GO:0072089	stem cell proliferation	0.25	0.73	0.60	---
	GO:0006096	glycolytic process	0.15	0.65	---	0.75
	GO:0006110	regulation of glycolytic process	0.22	0.54	---	0.66

b

Sample	chr	start	end	ID Holoclone	Annotation to genes	Gene symbol	Annotation to regulatory elements	Recovered in PGc
PGc	chr5	131410002	131410003	PGc_H1	Intron	CSF2	no mark	no
	chr2	144859325	144859326	PGc_H2	Intron	GTDC1	no mark	no
	chr4	101941589	101941590	PGc_H3	Intergenic	-	weak enhancer	no
	chr4	39355299	39355300	PGc_H4	Intron	RFC1	weak enhancer	no
	chr19	17908000	17908001	PGc_H5	Intron	B3GNT3	no mark	no
	chr19	42615156	42615157	PGc_H6	Intron	POU2F2	no mark	no
	chr5	150977858	150977859	PGc_H7*	Intergenic	-	active enhancer	yes
	chr17	80832738	80832739	PGc_H7*	Intron	TBCD	active enhancer	yes
	chr16	56726522	56726523	PGc_H7*	Intergenic	-	no mark	yes
	chr2	8999619	8999620	PGc_H8	Intron	MBOAT2	no mark	no
	chr3	47024025	47024026	PGc_H9	Promoter	CCDC12	active promoter	yes
	chrY	18367597	18367598	PGc_H10	Intergenic	-	no mark	no
	chr6	160458524	160458525	PGc_H11	Intron	IGF2R	no mark	no
	chr14	917111334	917111335	PGc_H12	Promoter	GPR68	active promoter	yes
	chr11	13946563	13946564	PGc_H13	Promoter	LOC101928132	no mark	yes
4Mc	chr14	33789922	33789923	PGc_H14	Intron	NPAS3	no mark	no
	chr13	20693331	20693332	PGc_H15	Intergenic	-	weak enhancer	no
	chr6	136930722	136930723	PGc_H16	Intron	MAP3K5	weak enhancer	yes
	chr18	65398639	65398640	PGc_H17	Intron	LOC643542	no mark	no
	chr4	11625725	11625726	PGc_H18	Intergenic	-	active enhancer	no
	chr20	22743911	22743912	PGc_H19	Intergenic	-	no mark	yes
	chr8	48293010	48293011	PGc_H20	Intron	SPIDR	active enhancer	no
	chr1	183130951	183130952	4Mc_H1-11**	Intergenic	-	no mark	yes
	chr9	103188807	103188808	4Mc_H1-11**	Promoter	MSANTD3	active promoter	yes
	chr14	105213201	105213202	4Mc_H12	Intron	ADSSL1	no mark	no
8Mc ₁	chr15	39577423	39577424	4Mc_H13	Intergenic	-	no mark	yes
	chr8	67025314	67025315	8Mc ₁ _H1-2	Intergenic	-	active enhancer	yes
	chr9	125129763	125129764	8Mc ₁ _H3	Promoter	PTGS1	no mark	yes
	chr17	76158277	76158278	8Mc ₁ _H4-5	Intron	C17orf99	no mark	no
	chrX	114601642	114601643	8Mc ₁ _H6	Intergenic	-	no mark	yes
8Mc ₂	chr5	135342207	135342208	8Mc ₁ _H7	Intergenic	-	no mark	yes

a. Enrichment of cancer-related biological process in genes harbouring an insertion. Statistically significant enrichments at a 95% confidence level ($q \leq 0.05$ in Fisher's exact test) are in bold. GO categories were selected to represent the cancer hallmarks described in ref. 16. **b.** Genomic and functional annotations of integrations in holoclones.

Extended Data Table 2 | Clonal analysis was performed on pre-graft cultures (PGc), a graft ready for transplantation (Graft) and on primary cultures established at 4 (4Mc) and 8 (8Mc₁) months after grafting

ID sample	ID-Replicate	Total number of clones	H	M/P	H Frequency (%)
PGc	PG-1	88	10	78	11.36
	PG-2	63	4	59	6.35
	PG-3	62	3	59	4.84
	PG-4	66	3	63	4.55
Total		279	20	259	7.17
Graft	Graft	95	4	91	4.21
	4Mc-1	121	8	113	6.61
	4Mc-2	105	5	100	4.76
	4Mc-3	52	1	51	1.92
Total		278	14	264	5.04
8Mc₁	8Mc ₁ -1	56	4	52	7.14
	8Mc ₁ -2	74	3	71	4.05
	Total	130	7	123	5.38

H, M and P indicate holoclones, meroclones and paraclonies, respectively. Frequency indicates the percentage of holoclones detected in the population of clonogenic keratinocytes. Graft was not used for LAM-PCR or NGS analyses but for holoclone quantification as part of quality control.